J|A|C|S
ARTICLES
Published on Web 04/29/2004

# Mechanism of Palladium-Catalyzed Diene Cyclization/Hydrosilylation: Direct Observation of Intramolecular Carbometalation

Nicholas S. Perch and Ross A. Widenhoefer*

*Contribution from the P. M. Gross Chemical Laboratory, Duke University, Durham, North Carolina 27708-0346*

Received January 12, 2004; E-mail: rwidenho@chem.duke.edu

***Abstract:*** The results of kinetic, deuterium-labeling, and low-temperature NMR studies have established a mechanism for the palladium-catalyzed cyclization/hydrosilylation of dimethyl diallylmalonate (**1**) with triethylsilane involving rapid, irreversible conversion of the palladium silyl complex $[(phen)Pd(SiEt_3)(NCAr)]^+$ $[BAr_4]^-$ [Ar = 3,5-$C_6H_3(CF_3)_2$] (**4b**) and **1** to the palladium 5-hexenyl chelate complex $\{(phen)Pd[\eta^1,\eta^2\text{-}CH(CH_2SiEt_3)CH_2C(CO_2Me)_2CH_2CH{=}CH_2]\}^+$ $[BAr_4]^-$ (**5**), followed by intramolecular carbometalation of **5** to form the palladium cyclopentylmethyl complex *trans*-$\{(phen)Pd[CH_2CHCH_2C(CO_2Me)_2CH_2CHCH_2SiEt_3]\text{-}(NCAr)\}^+$ $[BAr_4]^-$ (**6**), and associative silylation of **6** to release **3** and regenerate **4b**.

## Introduction

Functionalized carbocycles are among the most common structural components of naturally occurring and/or biologically active molecules and, for this reason, considerable effort has been directed toward the development of general and efficient methods for the synthesis of functionalized carbocycles.[1] Transition metal-catalyzed methods have demonstrated particular utility in the synthesis of functionalized carbocycles due to the ability of transition metal complexes to facilitate transformations not possible using traditional approaches and due to the high levels of selectivity, efficiency, and atom-economy often realized via transition metal catalysis.[2] Notable among these transition metal-catalyzed carbocyclization processes are the cyclization/addition of enynes,[3,4] dienes,[5,6] diynes,[7,8] or bis(dienes)[9] with a hydrosilane, hydrostannane, or bimetallic reagent to form a carbocycle that possesses one or more functionalized C−X bonds that can be manipulated in a subsequent transformation.[10]

We have developed a number of effective transition metal-catalyzed cyclization/addition protocols,[4,6,8] including the palladium-catalyzed cyclization/hydrosilylation of functionalized 1,6-dienes to form silylated cyclopentanes.[6] For example, reaction of dimethyl diallylmalonate (**1**) and $HSiEt_3$ catalyzed by $[(phen)Pd(Me)(OEt_2)]^+$ $[BAr_4]^-$ [Ar = 3,5-$C_6H_3(CF_3)_2$] (**2a**) (5 mol %) at 0 °C for 5 min formed silylated cyclopentane **3** in 92% isolated yield with ≥98% trans selectivity (Scheme 1).[11] This protocol displayed good functional group compatibility, high regio- and diastereoselectivity, and low air- and moisture-sensitivity and was applicable to the synthesis of cyclohexanes, fused and tethered polycyclic compounds, and nitrogen heterocycles.[6] A notable extension of this chemistry was the asymmetric cyclization/hydrosilylation of 1,6-dienes catalyzed by enantiomerically pure palladium pyridine-oxazoline complexes to form silylated cyclopentanes with up to 95% ee.[6]

In contrast to our thorough exploration of the scope, limitations, and extensions of palladium-catalyzed diene cyclization/hydrosilylation,[6] we have generated little information regarding the mechanism of this transformation, nor has detailed information regarding the mechanism of a late transition metal-catalyzed cyclization/addition process been reported. Although the mechanisms of zirconocene-catalyzed diene carboalumination[12] and

(1) (a) Hudlicky, T.; Price, J. D. *Chem. Rev.* **1989**, *89*, 1467. (b) Trost, B. M. *Chem. Soc. Rev.* **1982**, *11*, 141.
(2) (a) Ojima, I.; Tzamarioudaki, M.; Li, Z.; Donovan, R. J. *Chem. Rev.* **1996**, *96*, 635. (b) Lautens, M.; Klute, W.; Tam, W. *Chem. Rev.* **1996**, *96*, 49. (c) Trost, B. M. *Angew. Chem., Int. Ed. Engl.* **1995**, *34*, 259.
(3) (a) Ojima, I.; Donovan, R. J.; Shay, W. R. *J. Am. Chem. Soc.* **1992**, *114*, 6580. (b) Muraoka, T.; Matsuda, I.; Itoh, K. *Tetrahedron Lett.* **1998**, *39*, 7325. (c) Ojima, I.; Vu, A. T.; Lee, S.-L.; McCullagh, J. V.; Moralee, A. C.; Fujiwara, M.; Hoang, T. H. *J. Am. Chem. Soc.* **2002**, *124*, 9164. (d) Molander, G. A.; Retsch, W. H. *J. Am. Chem. Soc.* **1997**, *119*, 8817.
(4) Chakrapani, H.; Liu, C.; Widenhoefer, R. A. *Org. Lett.* **2003**, *5*, 157.
(5) (a) Negishi, E.-i.; Jensen, M. D.; Kondakov, D. Y.; Wang, S. *J. Am. Chem. Soc.* **1994**, *116*, 8404. (b) Shaughnessy, K. H.; Waymouth, R. M. *J. Am. Chem. Soc.* **1995**, *117*, 5873. (c) Molander, G. A.; Hoberg, J. O. *J. Am. Chem. Soc.* **1992**, *114*, 3123. (d) Onozawa, S.; Sakakura, T.; Tanaka, M. *Tetrahedron Lett.* **1994**, *35*, 8177. (e) Molander, G. A.; Nichols, P. J. *J. Am. Chem. Soc.* **1995**, *117*, 4415. (f) Molander, G. A.; Dowdy, E. D.; Schumann, H. *J. Org. Chem.* **1998**, *63*, 3386. (g) Molander, G. A.; Corrette, C. P. *J. Org. Chem.* **1999**, *64*, 9697.
(6) Widenhoefer, R. A. *Acc. Chem. Res.* **2002**, *35*, 905.
(7) (a) Tamao, K.; Kobayashi, K.; Ito, Y. *J. Am. Chem. Soc.* **1989**, *111*, 6478. (b) Tamao, K.; Kobayashi, K.; Ito, Y. *Synlett* **1992**, 539.
(8) (a) Madine, J. W.; Wang, X.; Widenhoefer, R. A. *Org. Lett.* **2001**, *3*, 385. (b) Wang, X.; Chakrapani, H.; Madine, J. W.; Keyerleber, M. A.; Widenhoefer, R. A. *J. Org. Chem.* **2002**, *67*, 2778. (c) Liu, C.; Widenhoefer, R. A. *Organometallics* **2002**, *21*, 5666.
(9) (a) Obora, Y.; Tsuji, Y.; Kakehi, Kobayashi, M.; Shinkai, Y.; Ebihara, M.; Kawamura, T. *J. Chem. Soc., Perkin Trans. 1* **1995**, 599. (b) Takacs, J. M.; Chandramouli, S. *Organometallics* **1990**, *9*, 2877. (c) Takacs, J. M.; Zhu, J.; Chandramouli, S. *J. Am. Chem. Soc.* **1992**, *114*, 773.
(10) (a) These secondary transformations include the oxidation of organosilanes[10b] and organoboranes and the cross-coupling of alkenylsilanes,[10c] alkenylstannanes,[10d] and organoboranes.[10e] (b) Jones, G. R.; Landais, Y. *Tetrahedron* **1996**, *52*, 7599. (c) Hiyama, T.; Hatanaka, Y. *Pure Appl. Chem.* **1994**, *66*, 1471. (d) Mitchell, T. N. *Synthesis* **1992**, 803. (e) Suzuki, A. *Pure Appl. Chem.* **1991**, *63*, 419.
(11) DeCarli, M. A.; Widenhoefer, R. A. *J. Am. Chem. Soc.* **1998**, *120*, 3805.
(12) Shaughnessy, K. H.; Waymouth, R. M. *Organometallics* **1998**, *17*, 5728.


**10.1021/ja049806f CCC: $27.50** 

***Scheme 1***

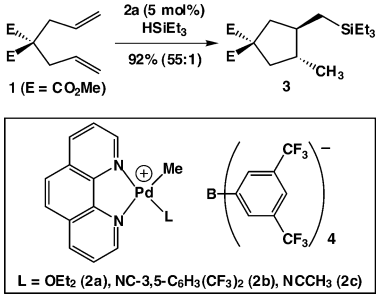


carbomagnesiation have been reported,[13] these systems are poor models for synthetically significant late transition metal-catalyzed cyclization/addition processes, including palladium-catalyzed diene cyclization/hydrosilylation. Rather, our mechanistic understanding of palladium-catalyzed diene cyclization/hydrosilylation has been restricted to insights gleaned from our synthetic investigations[6] or from the mechanistic studies of related palladium-catalyzed transformations including olefin hydrosilylation,[14] dimerization,[15] and copolymerization[16] and diene cycloisomerization.[17] Due to the synthetic potential of palladium-catalyzed diene cyclization/hydrosilylation specifically, and late transition metal-catalyzed cyclization/addition in general, we initiated a study directed toward elucidating the mechanism of palladium-catalyzed diene cyclization/hydrosilylation. Here we report a full account of our mechanistic investigation of the cyclization/hydrosilylation of **1** and $HSiEt_3$ to form **3** catalyzed by $[(phen)Pd(Me)(NCAr)]^+$ $[BAr_4]^-$ [Ar = 3,5-$C_6H_3(CF_3)_2$] (**2b**). This study has produced both the first detailed mechanism of a late transition metal-catalyzed cyclization/addition process and the first direct observation of the $\beta$-migratory insertion of a coordinated olefin into the M−C bond of a transition metal alkyl olefin chelate complex (intramolecular carbometalation).[18]

## Results

Brookhart has shown that the cationic palladium etherate complex **2a** reacts rapidly with $HSiEt_3$ at −80 °C to form the palladium silyl silane complex $[(phen)Pd(SiEt_3)(HSiEt_3)]^+$ $[BAr_4]^-$ [Ar = 3,5-$C_6H_3(CF_3)_2$] (**4a**), which reacts with simple olefins to form palladium silyl olefin complexes.[14] On the basis of these results, we initiated our mechanistic investigation of palladium-catalyzed diene cyclization/hydrosilylation with the stoichiometric reaction of dimethyl diallylmalonate (**1**) and the palladium silyl complex $[(phen)Pd(SiEt_3)(NCAr)]^+$ $[BAr_4]^-$ [Ar = 3,5-$C_6H_3(CF_3)_2$] (**4b**). Complex **4b** was employed in preference to **4a** to avoid potential complications arising from the silane ligand of **4a** and due to the enhanced thermal stability of **4b** relative to that of **4a**. Silyl complex **4b** was generated in quantitative yield (101 ± 10% by $^1H$ NMR) by treatment of a $CD_2Cl_2$ solution of **2b** (42 mM) with triethylsilane (1 equiv) at −81 °C for 5 min (Scheme 2). Conversion of **2b** to **4b** was established by the disappearance of the Pd−$CH_3$ resonance of

***Scheme 2***

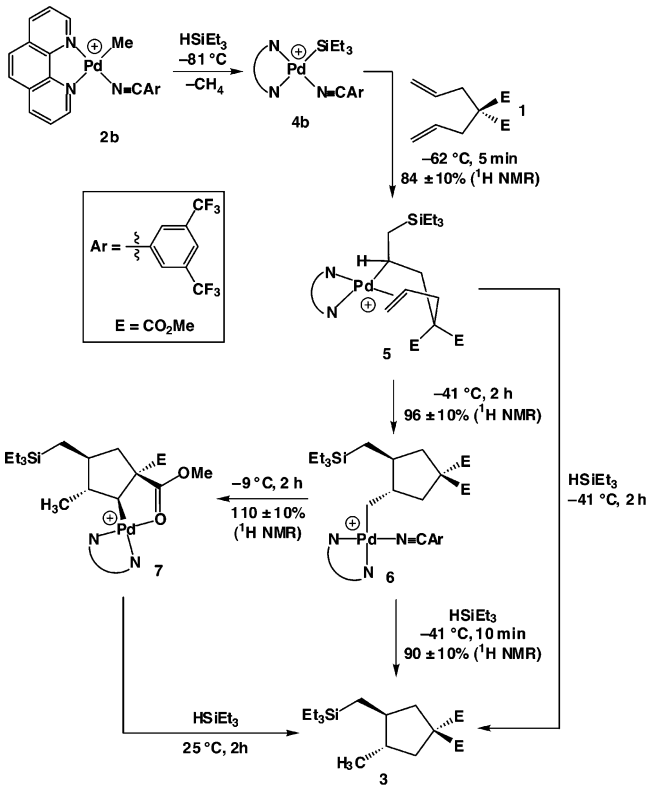


**2b** ($\delta$ 1.26) and by the appearance of the Pd−$SiEt_3$ resonances of **4b** [$\delta$ 0.97 (q), 1.06 (t), $J$ = 7.5 Hz] and free methane ($\delta$ 0.21) in the $^1H$ NMR spectrum.

**Formation of Alkyl Olefin Chelate Complex 5.** Addition of **1** (1 equiv) to a solution of **4b** (42 mM) at −62 °C led to rapid ($t_{1/2} \leq 5$ min) formation of the palladium 5-hexenyl chelate complex $\{(phen)Pd[\eta^1,\eta^2\text{-}CH(CH_2SiEt_3)CH_2C(CO_2Me)_2CH_2CH{=}CH_2]\}^+$ $[BAr_4]^-$ (**5**) in 84 ± 10% yield by $^1H$ NMR spectroscopy as a single diastereomer (Scheme 2).[19] Thermally sensitive **5** was characterized in solution at −62 °C by NMR spectroscopy. The $^1H$ NMR spectrum of **5** displayed a one-proton multiplet at $\delta$ 2.66 (Pd−C*H*), a one proton doublet of doublets at $\delta$ 1.23 ($J$ = 3, 13 Hz, −C*H*$HSiEt_3$), and a one-proton triplet at $\delta$ 1.11 ($J$ = 13 Hz, −CH*H*$SiEt_3$), which together established insertion of an olefin of **1** into the Pd−Si bond of **4b**. Olefin coordination was supported by the large difference of the $^1H$ NMR chemical shifts of the olefinic protons of **5** [$\delta$ 6.41 (dddd, $J$ = 4, 8, 9, 16 Hz), 5.44 (d, $J_{cis}$ = 9 Hz), and 4.22 (d, $J_{trans}$ = 16 Hz)] relative to the corresponding olefinic resonances of uncomplexed **1** [$\delta$ 5.53, 5.09, and 5.06]. Coordination of the pendant olefin of **5** was further supported by the large difference of the $^{13}C$ NMR chemical shifts of the olefinic carbons of the $^{13}C$-labeled isotopomer $\{(phen)Pd[\eta^1,\eta^2\text{-}{}^{13}CH(^{13}CH_2SiEt_3)^{13}CH_2C(CO_2Me)_2{}^{13}CH_2{}^{13}CH{=}{}^{13}CH_2]\}^+$ $[BAr_4]^-$ (**5**-$^{13}C_6$) ($\delta$ 103.7 and 87.5) relative to the corresponding olefinic resonances of uncomplexed **1**-1,2,3,5,6,7-$^{13}C_6$ ($\delta$ 131.4 and 119.7) and by the much smaller C=C coupling constant of **5**-$^{13}C_6$ ($J_{C=C}$ = 47 Hz) relative to free **1**-1,2,3,5,6,7-$^{13}C_6$ ($J_{C=C}$ = 69 Hz).[20]

(13) Knight, K. S.; Wang, D.; Waymouth, R. M.; Ziller, J. *J. Am. Chem. Soc.* **1994**, *116*, 1845.
(14) LaPointe, A. M.; Rix, F. C.; Brookhart, M. *J. Am. Chem. Soc.* **1997**, *119*, 906.
(15) Rix, F. C.; Brookhart, M. *J. Am. Chem. Soc.* **1995**, *117*, 1137.
(16) Rix, F. C.; Brookhart, M.; White, P. S. *J. Am. Chem. Soc.* **1996**, *118*, 4746.
(17) Goj, L. A.; Widenhoefer, R. A. *J. Am. Chem. Soc.* **2001**, *123*, 11290.
(18) A portion of these results have been communicated: Perch, N. S.; Widenhoefer, R. A. *Organometallics* **2001**, *20*, 5251.

(19) Neither formation of byproducts nor decomposition was observed in any of these transformations. The formation of **6** in 93% yield from **3** suggests that the yield for the conversion of **2** to **4** was higher than indicated by $^1H$ NMR.

(20) Benn, R.; Rufiñska, A. *J. Organomet. Chem.* **1982**, *238*, C27.

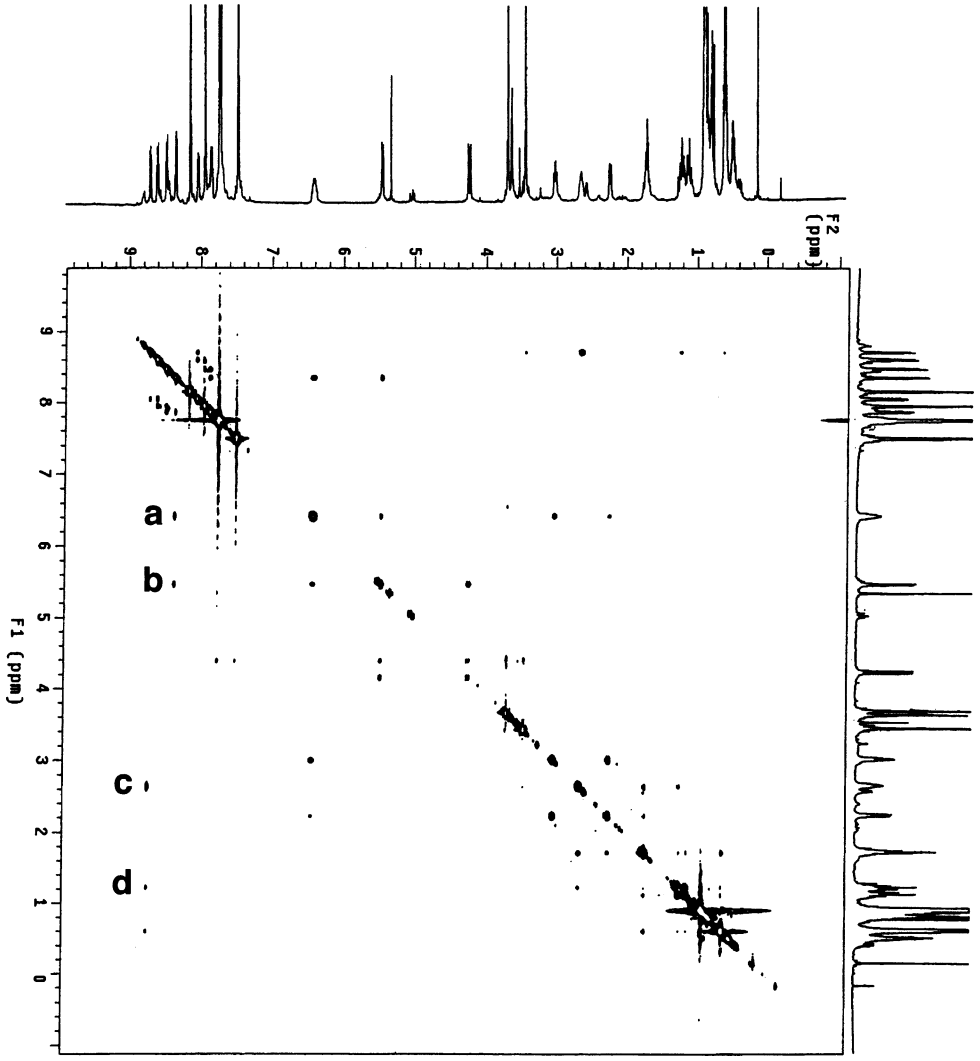


***Figure 1.*** $^1$H NOESY spectrum of **5**. Cross-peaks corresponding to through-space interactions between the ortho phenanthroline proton at $\delta$ 8.35 with the internal (a) and trans-terminal olefinic protons (b), and between the ortho phenanthroline proton at $\delta$ 8.71 with the Pd−C*H* methine (c), and the −C*H*HSiEt$_3$ methylene protons (d) are denoted.

Low-temperature $^1$H−$^1$H NOESY analysis of **5** revealed through-space interactions between the ortho phenanthroline proton at $\delta$ 8.35 with both the internal ($\delta$ 6.41) and trans-terminal olefinic protons ($\delta$ 5.44) (Figure 1). These interactions established orientation of the olefin approximately perpendicular to the coordination plane, as is typically observed with non-chelated square planar Pd(II) and Pt(II) olefin complexes.[21] NOESY analysis of **5** also revealed through-space interactions between the ortho phenanthroline proton at $\delta$ 8.71 with both the methine proton of the palladium-bound alkyl group ($\delta$ 2.66) and with one of the diastereotopic methylene protons of the exocyclic triethylsilylmethyl group ($\delta$ 1.11) (Figure 1). Analysis of molecular models indicated that interaction of the ortho phenanthroline proton with both the Pd−C*H* and −C*H*HSiEt$_3$ protons can be achieved only if the triethylsilylmethyl group adopts an axial or pseudoaxial position with respect to the hexenyl chelate. Although this result was initially somewhat surprising, further analysis of molecular models revealed that in an equatorial or pseudoequatorial position, the triethylsilylmethyl group experiences a pronounced, unfavorable interaction with the phenanthroline ligand. Given the axial orientation of the triethylsilylmethyl group, **5** likely adopts a boatlike conformation to avoid unfavorable 1,3-diaxial interaction between the triethylsilylmethyl group and one of the carbomethoxy groups.[22]

To probe for reversible formation of **5**, a solution of **5** (25 mM) that contained NCAr (25 mM) was treated with 4,4-dicarbomethoxy-2,6-dideuterio-1,7-heptadiene (**1**-2,6-$d_2$) (50 mM) and monitored periodically by $^1$H NMR spectroscopy. Formation of neither free **1** nor **5**-$d_2$ was detected after 90 min at −80 °C and 30 min at −60 °C, which established irreversible conversion of **4b** to **5** under these conditions. In a similar manner, $^1$H NMR analysis of solutions of **5** that contained either NCAr (42 mM) or both NCAr (42 mM) and **1** (42 mM) at −62 °C revealed no evidence for displacement of the chelated olefin of **5** to form the 5-hexenyl species **5-L** (L = NCAr, **1**) (Scheme 3). The failure to form detectable quantities of **5-L** under these

(21) Albright, T. A.; Hoffmann, R.; Thibeault, J. C.; Thorn, D. L. *J. Am. Chem. Soc.* **1979**, *101*, 3801 and ref 23 therein.

(22) We cannot rule out a structure for **5** in which the α-(triethylsilyl)methyl group and the terminus of the complexed olefin have a cis relationship. However, if this were the case, cis to trans isomerization must precede conversion of **5** to **6**, and this isomerization must be fast relative to the conversion of **5** to **6** as the rate of conversion of **5** to **6** was independent of [NCAr].

***Scheme 3***

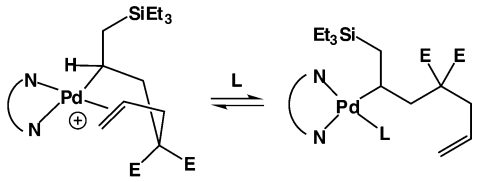


**5** **5-L (L = NCAr or 1)**

***Table 1.*** First-Order Rate Constants for the Conversion of **5** ($[\mathbf{5}]_0$ = 42 mM) to **6** in $CD_2Cl_2$ as a Function of Temperature

| entry | temp (°C) | $(10^4)k_{\mathbf{5}\rightarrow\mathbf{6}}(s^{-1})$ |
|---|---|---|
| 1 | −62 | 0.288 ± 0.022 |
| 2 | −55 | 0.711 ± 0.002 |
| 3 | −51 | 1.41 ± 0.01 |
| 4 | −41 | 5.04 ± 0.05 |
| 5 | −41 | 4.35 ± 0.03 |
| 6 | −41 | 6.33 ± 0.04 |
| 7 | −30 | 27.2 ± 0.5 |

conditions is not surprising, given the likelihood of a large negative entropy of reaction for the conversion of **5** to **5-L**,[16,23,24] and does not rule out rapid and reversible formation of **5-L**. To the contrary, given the extreme facility of the associative exchange of ethylene and α-olefins at cationic square planar palladium complexes,[14−16,25,26] reversible formation of **5-L** from **5** in the presence of **1** or NCAr appears likely. Because the relative stereochemistry of **5** is lost upon olefin displacement, the diastereoselective formation of **5** is likely under thermodynamic control.

**Formation of Palladium Cyclopentylmethyl Complex 6.** Warming a solution of palladium alkyl olefin chelate complex **5** at −41 °C for 2 h led to *β*-migratory insertion and formation of the palladium cyclopentylmethyl complex *trans*-{(phen)Pd-[$CH_2$CHC$H_2$C($CO_2$Me)$_2$C$H_2$CHC$H_2$Si$Et_3$](NCAr)}$^+$ [$BAr_4$]$^-$ (**6**) in 96 ± 10% yield by $^1$H NMR spectroscopy as a single diastereomer (Scheme 2). Thermally sensitive **6** was characterized in solution by $^1$H- and $^{13}$C NMR spectroscopy at −41 °C. The $^1$H NMR spectrum of **6** displayed two one-proton multiplets at *δ* 1.67 and 1.80, assigned to the cyclopentyl methine protons, and two one-proton doublets of doublets at *δ* 2.09 ($J$ = 8, 11 Hz) and 2.52 ($J$ = 4, 8 Hz), assigned to the palladium-bound methylene group, which together established *β*-migratory insertion and cyclopentyl ring formation. The trans stereochemistry of **6** was established by the exclusive formation of *trans*-**3** from reaction of **6** with $HSiEt_3$, given the likelihood that conversion of **5** to **6** is irreversible under reaction conditions (see below).

Disappearance of **5** (∼42 mM) at −41 °C in the presence of NCAr (∼42 mM) obeyed first-order kinetics to >3 half-lives with a rate constant of $k = 5.2 \pm 0.8 \times 10^{-4}$ s$^{-1}$; $\Delta G^{\ddagger}_{232\ K} = 16.9 \pm 0.1$ kcal mol$^{-1}$, as the average of three separate experiments (Table 1, entries 4−6; Figure 2). Because NCAr was completely consumed during the conversion of **5** to **6**, the first-order decay of **5** established the zero-order dependence of the rate of conversion of **5** to **6** on [NCAr]. First-order rate

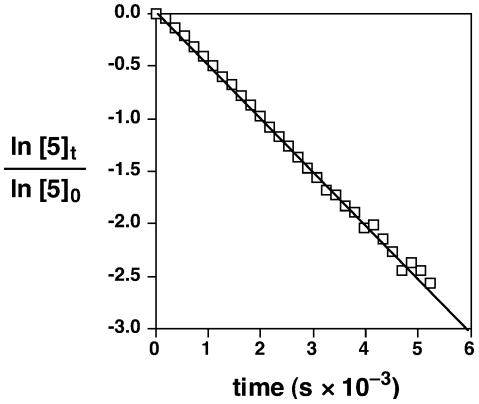


***Figure 2.*** First-order plot for the conversion of **5** ($[\mathbf{5}]_0$ = 42 mM) to **6** at −41 °C in $CD_2Cl_2$ that contained NCAr (42 mM).

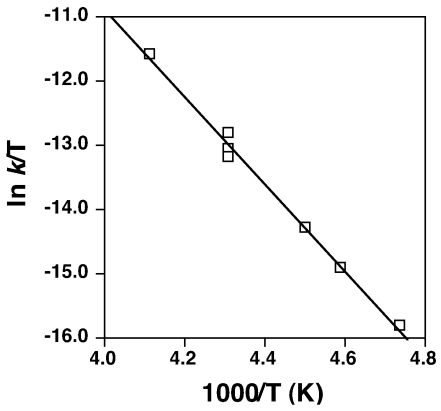


***Figure 3.*** Eyring plot for the conversion of **5** to **6** over the temperature range −30 to −62 °C.

constants for the conversion of **5** to **6** were determined as a function of temperature from −30 to −62 °C (Table 1). An Eyring plot of these data provided the activation parameters for the conversion of **5** to **6** (Figure 3): $\Delta H^{\ddagger} = 13.5 \pm 0.6$ kcal mol$^{-1}$ and $\Delta S^{\ddagger} = -15 \pm 2$ eu.

**Conversion of 6 to Palladium Carbonyl Chelate Complex 7.** Warming a solution of palladium cyclopentylmethyl complex **6** at −9 °C for 2 h in the absence of silane led to rearrangement and formation of the thermally stable cyclopentyl carbonyl chelate complex *trans,trans*-{(phen)Pd[CHCH(Me)CH($CH_2$-Si$Et_3$)$CH_2$C(COOMe)(COOMe)]}$^+$ [$BAr_4$]$^-$ (**7**) in 110 ± 10% yield (93 ± 10% from **4b**) by $^1$H NMR spectroscopy as a single diastereomer (Scheme 2).[19] Complex **7** was subsequently isolated in 49% yield from the preparative-scale reaction of an equimolar mixture of [(phen)Pd(Me)(N$CCH_3$)]$^+$ [$BAr_4$]$^-$ (**2c**), **1**, and $HSiEt_3$ and was characterized by spectroscopy and elemental analysis. The $^1$H NMR spectrum of **7** displayed a one-proton doublet at *δ* 2.47 ($J$ = 10.5 Hz, Pd−C*H*) and a three-proton doublet at *δ* 1.20 ($J$ = 6.5 Hz, CH−C$H_3$), which together established migration of the palladium atom from the exocyclic methylene carbon to the C(2) carbon atom of the cyclopentyl ring. The relative stereochemistry of **7** was established by degradation with $DSiEt_3$ (see below) and by comparison of the $^1$H NMR spectrum of **7** to that of the structurally characterized analogue *trans,trans*-{(phen)Pd[CHCH(Me)CH(Et)$CH_2$C-

(23) Johnson, L. K.; Mecking, S.; Brookhart, M. *J. Am. Chem. Soc.* **1996**, *118*, 267.
(24) Mecking, S.; Johnson, L. K.; Wang, L.; Brookhart, M. *J. Am. Chem. Soc.* **1998**, *120*, 888.
(25) Johnson, L. K.; Killian, C. M.; Brookhart, M. *J. Am. Chem. Soc.* **1995**, *117*, 6414.
(26) Rix, F. C.; Brookhart, M.; White, P. S. *J. Am. Chem. Soc.* **1996**, *118*, 2436.

***Scheme 4***

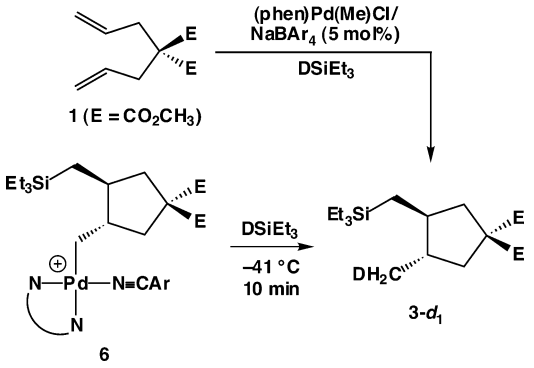


$(COOMe)(COOMe)]\}^+ [BAr_4]^-$ (**7a**).[17] Conversion of palladium cyclopentylmethyl complex **6** to palladium carbonyl chelate complex **7** did not obey first-order kinetics (Figure S1), presumably due to the increasing concentration of free NCAr with increasing conversion.

**Silylation of Palladium Alkyl Complexes.** Reaction of palladium cyclopentylmethyl complex **6** (32 mM) with triethylsilane (50 mM) at −41 °C for 10 min led to complete (≥95%) consumption of **6** to form a 1:1 mixture of the silylated carbocycle **3** and palladium silyl complex **4b** as the exclusive products in 90 ± 10% yield by $^1$H NMR spectroscopy (Scheme 2). Assuming that silylation of **6** obeyed a second-order rate law, as was established for the silylation of **7** (see below), we estimate a lower limit for the second-order rate constant for the silylation of **6** of $k \geq 0.19$ M$^{-1}$ s$^{-1}$ at −41 °C ($\Delta G^{\ddagger} \leq 14.2$ kcal mol$^{-1}$).[27] Although the extreme facility of this transformation precluded detailed kinetic analysis, silylation of **6** was inhibited by excess nitrile, and reaction of **6** (40 mM) and $HSiEt_3$ (50 mM) in the presence of $CD_3CN$ (0.5 M) required ≥30 min to reach completion at 0 °C. Reaction of **6** with $DSiEt_3$ at −41 °C formed 1,1-dicarbomethoxy-3-deuteriomethyl-4-triethysilylmethylcyclopentane (**3**-$d_1$) as the exclusive isotopomer as determined by $^{13}$C NMR and GC/MS analysis (Scheme 4). Selective incorporation of deuterium into the exocyclic methyl group of **3**-$d_1$ was established by the 1:1:1 triplet at $\delta$ 17.1 ($J$ = 19.1 Hz, isotopic shift = 300 ppb), corresponding to the exocyclic $-CH_2D$ group in the $^{13}$C NMR spectrum. Noteworthy is that catalytic cyclization/deuteriosilylation of **1** with $DSiEt_3$ also formed **3**-$d_1$ as the exclusive isotopomer (Scheme 4).

Treatment of palladium alkyl olefin chelate complex **5** with $HSiEt_3$ formed none of the product resulting from silylation of the Pd−C bond of **5** but instead formed silylated carbocycle **3** as the exclusive organic product (Scheme 2). This result is in accord with the failure to form significant amounts (≤2%) of silylated uncyclized products in the palladium-catalyzed cyclization/hydrosilylation of **1** and $HSiEt_3$.[11] Reaction of **5** (43 mM) with $HSiEt_3$ (128 mM) to form **3** at −51 °C obeyed first-order kinetics to >2 half-lives with a rate constant of $k = 1.59 \pm 0.01 \times 10^{-4}$ s$^{-1}$ (Figure S2), which does not differ significantly from the first-order rate constant for the conversion of **5** to **6** at −51 °C ($k = 1.41 \pm 0.01 \times 10^{-4}$ s$^{-1}$) (Table 1, entry 3). These observations are consistent with conversion of **5** to **3** via rate-limiting conversion of **5** to **6** followed by rapid silylation of **6** to give **3**.

(27) (a) The rate constant $k$ for the silylation of **6** was calculated for the rate law: rate = $k$[**6**][$HSiEt_3$] employing the following equation: $kt = \{1/([HSiEt_3]_0 - [\mathbf{6}]_0)\} \times \ln\{([\mathbf{6}]_0 \times [HSiEt_3]_t)/([HSiEt_3]_0 \times [\mathbf{6}]_t)\}$, where $t$ = 600 s, $[\mathbf{6}]_0 = 0.032$ M, $[HSiEt_3]_0 = 0.050$ M, $[\mathbf{6}]_t = 0.0016$ M (95% conversion) $[HSiEt_3]_t = 0.0196$ M (95% conversion).[27b] (b) Frost, A. A.; Pearson, R. G. *Kinetics and Mechanism*; Wiley: New York, 1961; p 16.

***Table 2.*** Silane Concentration Dependence of the Rate of Conversion of **7** ($[\mathbf{7}]_0 = 20-36$ mM) to **3** at −14 °C in $CD_2Cl_2$

| entry | $[HSiEt_3]$ (M) | $(10^4)k_{obs}$ (s$^{-1}$) |
|---|---|---|
| 1 | 0.18 | 0.59 ± 0.01 |
| 2 | 0.20 | 0.50 ± 0.01 |
| 3 | 0.36 | 1.33 ± 0.01 |
| 4 | 0.38 | 1.45 ± 0.02 |
| 5 | 0.93 | 2.94 ± 0.05 |
| 6 | 0.93 | 3.0 ± 0.2 |
| 7 | 0.93 | 2.38 ± 0.03 |

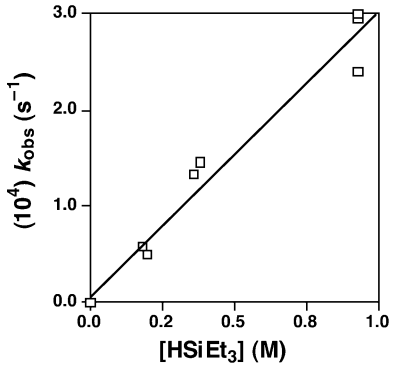


***Figure 4.*** Plot of $k_{obs}$ versus silane concentration for the reaction of **7** ($[\mathbf{7}]_0 = 20-36$ mM) and $HSiEt_3$ in $CD_2Cl_2$ at −14 °C.

***Scheme 5***

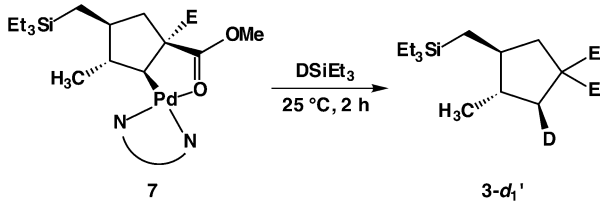


In contrast to the facile silylation of cyclopentylmethyl complex **6**, reaction of palladium carbonyl chelate complex **7** (30 mM) with $HSiEt_3$ (40 mM) to form **3** as the exclusive organic product required 2 h at room temperature (Scheme 2). Conversion of **7** (36 mM) to **3** at −14 °C in the presence of a large excess of $HSiEt_3$ (0.36 M) obeyed pseudo-first-order kinetics through ≥4 half-lives with an observed rate constant of $k_{obs} = 1.33 \pm 0.01 \times 10^{-4}$ s$^{-1}$ (Table 2, entry 3, Figure S3). To determine the dependence of the rate of the silylation of **7** on silane concentration, pseudo-first-order rate constants for reaction of **7** and $HSiEt_3$ at −14 °C were determined as a function of silane concentration from 0.18 to 0.93 M (Table 2). A linear plot of $k_{obs}$ versus $[HSiEt_3]$ established the first-order dependence of the rate of the conversion of **7** to **3** on silane concentration and the second-order rate law: rate = $k$[**7**][$HSiEt_3$], where $k = 3.3 \pm 0.3 \times 10^{-4}$ M$^{-1}$ s$^{-1}$ at 22 °C ($\Delta G^{\ddagger}_{259K} = 22.0 \pm 0.1$ kcal mol$^{-1}$) (Figure 4).

Treatment of **7** with $DSiEt_3$ (0.42 M) at room temperature for 2 h led to formation of *trans*,*trans*-1,1-dicarbomethoxy-2-deuterio-4-(triethylsilylmethyl)-3-methylcyclopentane (**3**-$d_1'$) in 46% yield with 83% isotopic purity as determined by GC/MS analysis (Scheme 5). The regiochemistry of **3**-$d_1'$ was established by the 1:1:1 triplet at $\delta$ 42.0 ($J_{CD}$ = 20.6 Hz, isotopic shift = 320 ppb), assigned to the C(2) carbon atom of the cyclopentane

***Table 3.*** Ratio of Silylated Cyclopentanes Formed from Reaction of **1** with a Mixture of $HSiEt_3$ (5 equiv) and $HSiMe_2R$ (R = Et, *n*-octyl, $OSiMe_3$, and Ph) (5 equiv) (entries 1−4) or with a Mixture of $HSiMe_2Ph$ (5 equiv) and $HSiMe_2(4\text{-}C_6H_4R)$ (R = $NMe_2$, OMe, F, and $CF_3$) (5 equiv) (entries 5−8) Catalyzed by **2b** (5 mol %) in DCE at Room Temperature

| entry | base silane | $HSiMe_2R$ | carbocycle $-SiMe_2R$ | **3**:**3a**–**3d** | **3d**:**3e**–**3h** |
|---|---|---|---|---|---|
| 1 | $HSiEt_3$ | Et | **3a** | 1:5.9 | − |
| 2 | $HSiEt_3$ | *n*-octyl | **3b** | 1:4.1 | − |
| 3 | $HSiEt_3$ | $OSiMe_3$ | **3c** | 1:48 | − |
| 4 | $HSiEt_3$ | Ph | **3d** | 1:15 | − |
| 5 | $HSiMe_2Ph$ | $4\text{-}C_6H_4NMe_2$ | **3e** | − | 1:3.2 |
| 6 | $HSiMe_2Ph$ | $4\text{-}C_6H_4OMe$ | **3f** | − | 1:1.7 |
| 7 | $HSiMe_2Ph$ | $4\text{-}C_6H_4F$ | **3g** | − | 2.7:1 |
| 8 | $HSiMe_2Ph$ | $4\text{-}C_6H_4CF_3$ | **3h** | − | 6.1:1 |

ring in the $^{13}C$ NMR spectrum. The relative stereochemistry of **3**-$d_1'$ was established by the absence of the doublet of doublets at $\delta$ 2.48 in the $^1H$ NMR spectrum of **3**-$d_1'$ that had been previously assigned to the methylene proton trans to the methyl group via two-dimensional $^1H-^1H$ COSY and NOESY spectroscopy of unlabeled **3**.

Two sets of experiments were performed to probe the effect of silane structure on the silyl-incorporation step in the catalytic cyclization/hydrosilylation of **1**. In one set of experiments, **1** was treated with a catalytic amount of **2b** and an excess of an equimolar mixture of $HSiEt_3$ (5 equiv) and $HSiMe_2R$ (R = Et, *n*-octyl, $OSiMe_3$, or Ph) (5 equiv) in 1,2-dichloroethane (DCE) to form a mixture of carbocycles **3** and **3a**, **3b**, **3c**, or **3d**, respectively (Table 3, entries 1−4). These data revealed that the extent of silane incorporation increased with both the decreasing steric bulk and increasing electron density of the silane. As examples, palladium-catalyzed reaction of **1** with a 1:1 mixture of $HSiEt_3$ and $HSiMe_2Et$ formed a 1:5.9 mixture of carbocycles **3**:**3a** (Table 3, entry 1), while reaction of **1** with a 1:1 mixture of $HSiEt_3$ and the small, electron-rich pentamethyldisiloxane formed a 1:48 mixture of carbocycles **3**:**3c** (Table 3, entry 3). To better quantify the effect of the electron density of the silane on the silyl-incorporation step in the catalytic cyclization/hydrosilylation of **1**, **1** was treated with a catalytic amount of **2b** and a mixture of $HSiMe_2Ph$ (5 equiv) and $HSiMe_2(4\text{-}C_6H_4R)$ (R = $NMe_2$, OMe, F, or $CF_3$) (5 equiv) to form a mixture of carbocycles **3d** and **3e**, **3f**, **3g**, or **3h**, respectively (Table 3, entries 5−8). The corresponding plot of log **3d**:**3e**-**3h** versus the Hammett $\sigma$-parameter was roughly linear with a slope of $\rho = -1.1$ (Figure 5).[28]

**Kinetics of Catalytic Cyclization/Hydrosilylation.** We sought to establish the resting state and rate behavior of the catalytic cyclization/hydrosilylation of **1** and $HSiEt_3$ under conditions that approximated the relative and absolute concentrations of diene and silane employed in preparative-scale reactions. To this end, a solution of **1** ($[\mathbf{1}]_0$ = 85 mM), $HSiEt_3$ ($[HSiEt_3]_0$ = 0.16 M),[29] NCAr ([NCAr] = 42 mM), and a catalytic amount of **2b** ($[\mathbf{2b}]_0$ = 12 mM) in $CD_2Cl_2$ was monitored periodically by $^1H$ NMR spectroscopy at −41 °C.

(28) (a) Exner, O. in *Correlation Analysis in Chemistry; Recent Advances*; Chapman, N. B., Shorter, J., Eds.; Plenum: New York, 1978; pp 439−540. (b) Matsui, K.; Hepler, *Can. J. Chem.* **1974**, *52*, 2906.

(29) The principle source of error in our kinetic measurements was determination of catalyst concentration, which stemmed from the difficulty in accurately weighing **2b** into the NMR tube. Efforts to improve the accuracy of these measurements by employing stock solutions of **2b** were unsuccessful due to the short lifetime of **2b** in solution at ambient temperature.

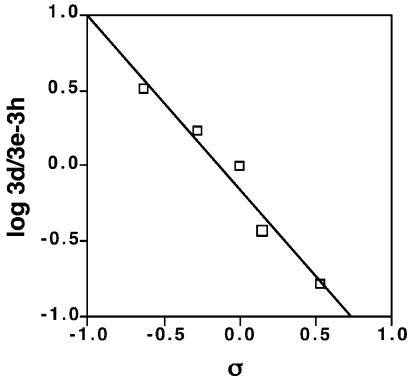


***Figure 5.*** Plot of log **3d**:**3e**−**3h** formed in the reaction of **1** with a 1:1 mixture of $HSiMe_2Ph$ (**3d**) and $HSiMe_2(4\text{-}C_6H_4R)$ [R = $NMe_2$ (**3e**), OMe (**3f**), F (**3g**), and $CF_3$ (**3h**)] catalyzed by **2b** versus the Hammet $\sigma$-parameter.[28]

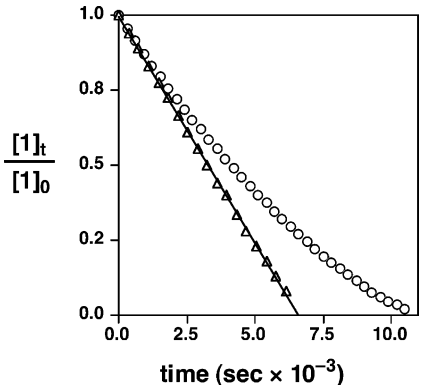


***Figure 6.*** Concentration versus time plots for the reaction of **1** ($[\mathbf{1}]_0$ = 85 mM) with $HSiEt_3$ catalyzed by **2b** ($[\mathbf{2b}]_0$ = 12 mM) at −41 °C in $CD_2Cl_2$ that contained NCAr (∼42 mM) where $[HSiEt_3]_0$ = 0.16 M (△) and 90 mM (○).

***Table 4.*** Observed Rate Constants for the Cyclization/Hydrosilylation of **1** ($[\mathbf{1}]_0$ = 85 mM) and $HSiEt_3$ ($[HSiEt_3]_0$ = 0.16 M) Catalyzed by **2b** in $CD_2Cl_2$ as a Function of Temperature, [**2b**], and [NCAr]

| entry | [**2b**] (mM) | temp (°C) | [NCAr] (mM) | $(10^6)\ k_{obs}$ ($M\ s^{-1}$) |
|---|---|---|---|---|
| 1 | 12 | −41 | 42 | 8.84 ± 0.09 |
| 2 | 12 | −41 | 42 | 8.20 ± 0.04 |
| 3 | 13 | −41 | 42 | 8.0 ± 0.2 |
| 4 | 12 | −41 | 12 | 7.42 ± 0.03 |
| 5 | 12 | −41 | 74 | 8.9 ± 0.1 |
| 6 | 6.0 | −41 | 42 | 3.93 ± 0.06 |
| 7 | 6.2 | −41 | 42 | 2.36 ± 0.02 |
| 8 | 24 | −41 | 42 | 19.5 ± 0.5 |
| 9 | 25 | −41 | 42 | 18.6 ± 0.3 |
| 10 | 12 | −25 | 42 | 26 ± 2 |
| 11 | 12 | −31 | 42 | 21.7 ± 0.3 |
| 12 | 13 | −51 | 42 | 1.08 ± 0.01 |
| 13 | 13 | −57 | 42 | 0.58 ± 0.01 |

Throughout complete conversion of **1** to **3**, alkyl olefin chelate complex **5** was the only palladium species detected by $^1H$ NMR spectroscopy. A plot of [**1**] versus time was linear to 3 half-lives with a pseudo-zero-order rate constant of $k_{obs}$ = 8.3 ± 0.6 × $10^{-6}$ $M\ s^{-1}$, determined as the average of three separate experiments (Figure 6, Table 4, entries 1−3).[29] The linear decay of [**1**] versus time established the zero-order dependence of the rate of conversion of **1** to **3** on [**1**] over the range 85−∼6 mM and on $[HSiEt_3]$ over the range 0.16−∼0.08 M. However, saturation kinetics were not maintained at lower silane concentration, and a plot of [**1**] versus time for reaction of **1** ($[\mathbf{1}]_0$ =

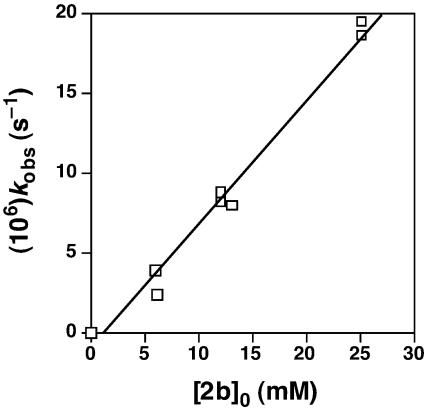


***Figure 7.*** Plot of $k_{obs}$ versus catalyst loading for the reaction of **1** ($[\mathbf{1}]_0$ = 85 mM) and $HSiEt_3$ ($[HSiEt_3]_0$ = 0.16 M) catalyzed by **2b** ($[\mathbf{2b}]_0$ = 12 mM) to form **3** at −41 °C in $CD_2Cl_2$.

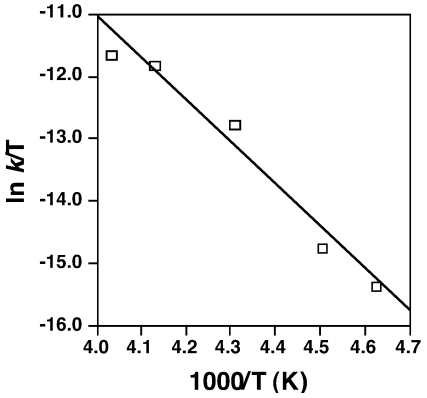


***Figure 8.*** Eyring plot for the reaction of **1** ($[\mathbf{1}]_0$ = 85 mM) and $HSiEt_3$ ($[HSiEt_3]_0$ = 0.16 M) catalyzed by **2b** ($[\mathbf{2b}]_0$ = 12 mM) over the temperature range −57 to −25 °C.

85 mM) and $HSiEt_3$ ($[HSiEt_3]_0$ = 90 mM) catalyzed by **2b** ($[\mathbf{2b}]_0$ = 12 mM) at −41 °C displayed pronounced positive curvature (Figure 6).[29] Point-by-point analysis of concentration versus time plots for catalytic cyclization/hydrosilylation of **1** ($[\mathbf{1}]_0$ = 85 mM) at low silane concentration ($[HSiEt_3]_0$ = 90 mM) indicated that the reaction rate decreased ∼50% as the silane concentration decreased from 90 to ∼5 mM (95% conversion).

The rate of palladium-catalyzed cyclization/hydrosilylation under saturation conditions was independent of nitrile concentration over the range of 12−74 mM (Table 4, entries 1−5). To determine the dependence of the rate of catalytic cyclization/hydrosilylation on catalyst concentration, pseudo-zero-order rate constants for reaction of **1** and $HSiEt_3$ ($[HSiEt_3]_0$ = 0.16 M) catalyzed by **2b** at −41 °C were determined as a function of precatalyst concentration (Table 4, entries 1−3, 6−9). A linear plot of $k_{obs}$ vs $[\mathbf{2b}]_0$ over the range of 0−25 mM established the first-order dependence of the rate of catalytic cyclization/hydrosilylation on precatalyst concentration and overall the first-order rate law under saturation conditions: rate = $k_{sat}[\mathbf{2b}]$, where $k_{sat} = 7.74 \pm 0.06 \times 10^{-4}$ $s^{-1}$; $\Delta G^{\ddagger} = 16.8 \pm 0.1$ kcal $mol^{-1}$ (Figure 7). Pseudo-zero-order rate constants for catalytic cyclization/hydrosilylation of **1** and $HSiEt_3$ ($[HSiEt_3]_0$ = 0.16 M) were measured as a function of temperature from −57 to −25 °C (Table 4, entries 1−3, and 10−13). An Eyring plot of the corresponding first-order rate constants provided the activation parameters: $\Delta H^{\ddagger} = 13 \pm 1$ kcal $mol^{-1}$ and $\Delta S^{\ddagger} = -15 \pm 3$ eu (Figure 8).

## Discussion

**Mechanism of Cyclization/Hydrosilylation.** The mechanism for the cyclization/hydrosilylation of **1** and $HSiEt_3$ catalyzed by **2b** to form **3** depicted in Scheme 6 is consistent with all of our experimental observations. Silylation of precatalyst **2b** with triethylsilane forms the observed palladium silyl complex **4b**. Displacement of the nitrile ligand of **4b** with one of the double bonds of **1** would form the unobserved palladium silyl olefin species **I**. $\beta$-Migratory insertion of the coordinated olefin into the Pd−Si bond of **I** to form the coordinatively unsaturated palladium alkyl intermediate **II** followed by coordination of the pendant olefin of **II** would form the observed alkyl olefin chelate complex **5**. $\beta$-Migratory insertion of the coordinated olefin into the Pd−C bond of **5** to generate the coordinately unsaturated palladium cyclopentylmethyl complex **III** followed by ligand capture with NCAr would form the observed palladium cyclopentylmethyl complex **6**. Associative silylation of **6** via the palladium−silane intermediate **IV** would release carbocycle **3** and regenerate the palladium silyl complex **4b**. Because cationic, coordinatively unsaturated palladium,[30−32] rhodium,[33] and cobalt[34,35] alkyl olefin complexes are stabilized by dynamic $\beta$-agostic interactions, coordinately unsaturated complexes **II** and **III** are also likely stabilized by $\beta$-agostic interactions.

**Conversion of 4b to 5.** The failure of alkyl olefin chelate complex **5** to exchange with **1**-2,6-$d_2$ at −60 °C established irreversible conversion of **4b** and **1** to **5**, which requires irreversibility in one or more of the microscopic steps in the conversion of **4b** to **5**. Because the nitrile ligand of catalyst precursor **2b** exchanges rapidly with a double bond of **1** at −80 °C ($K_{eq} \approx 0.25$),[36] it is likely that conversion of **4b** to **I** is also rapid and reversible. Although $\beta$-migratory insertion of ethylene into the Pd−Si bond of the cationic palladium silyl ethylene complex $[(phen)Pd(SiEt_3)(H_2C{=}CH_2)]^+$ is reversible at −60 °C,[14] we propose that rapid, exothermic coordination of the pendant olefin of **II** to form **5** renders both the conversion of **I** to **II** and the conversion of **II** to **5** irreversible. We estimate that conversion of **II** to **5** is exothermic by ∼12 kcal $mol^{-1}$ on the basis of DFT calculations for displacement of the $\beta$-agostic interaction of the palladium ethyl complex $[(H_2PCH{=}CHPH_2)PdCH_2CH_3]^+$ (**8**) with ethylene to form $[(H_2PCH{=}CHPH_2)Pd(H_2C{=}CH_2)(CH_2CH_3)]^+$ (**9**).[37] Irreversible silylpalladation of **1** with **4b** is further supported by the irreversible hydropalladation of **1** with a cationic palladium hydride complex.[17]

**Alkyl Olefin Chelate Complexes.** $\beta$-Migratory insertion of the coordinated olefin into the M−C bond of a transition metal alkyl olefin chelate complex is often invoked as the key C−C bond-forming process in transition metal-mediated and -catalyzed cyclization protocols.[2] Although $\beta$-migratory insertion of

(30) Temple, D. J.; Johnson, L. K.; Huff, R. L.; White, P. S.; Brookhart, M. *J. Am. Chem. Soc.* **2000**, *122*, 6686.
(31) Shultz, L. H.; Temple, D. J.; Brookhart, M. *J. Am. Chem. Soc.* **2001**, *123*, 11539.
(32) (a) Shultz, L. H.; Brookhart, M. *Organometallics* **2001**, *20*, 3975. (b) Temple, D. J.; Brookhart, M. *Organometallics* **1998**, *17*, 2290.
(33) Hauptman, E.; Sabo-Etienne, S.; White, P. S.; Brookhart, M.; Garner, J. M.; Fagan, P. J.; Calabrese, J. C. *J. Am. Chem. Soc.* **1994**, *116*, 8038.
(34) Brookhart, M.; Volpe, A. F.; Lincoln, D. M.; Horvath, I. T.; Millar, J. M. *J. Am. Chem. Soc.* **1990**, *112*, 5634.
(35) (a) Brookhart, M.; Lincoln, D. M.; Bennett, M. A.; Pelling, S. *J. Am. Chem. Soc.* **1990**, *112*, 2691. (b) Brookhart, M.; Grant, B. E. *J. Am. Chem. Soc.* **1993**, *115*, 2151.
(36) Perch, N. S.; Widenhoefer, R. A. Unpublished results.
(37) Margl, P.; Ziegler, T. *J. Am. Chem. Soc.* **1996**, *118*, 7337.

**Scheme 6**

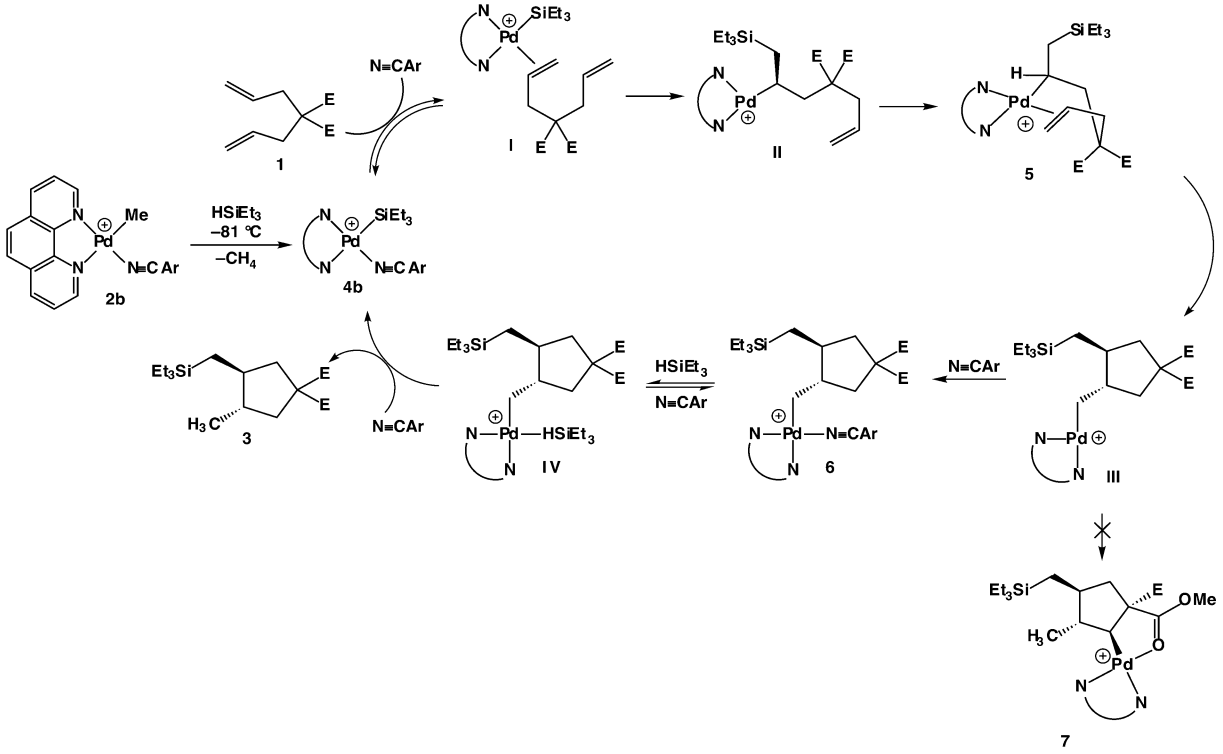


**Scheme 7**

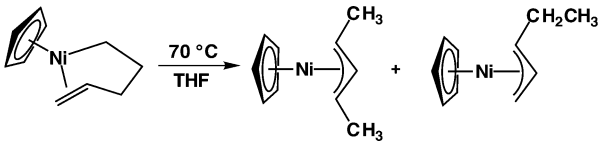


the coordinated olefin into the M−C bond of a nonchelated transition metal alkyl olefin complex has been directly observed,[15,16,25,26,30,31,34,35,38,39] olefin $\beta$-migratory insertion of the coordinated olefin into the M−C bond of a transition metal alkyl olefin chelate complex has not. Rather, the majority of well-characterized transition metal alkyl olefin chelate complexes decompose via $\beta$-hydride elimination without undergoing $\beta$-migratory insertion.[40] For example, the nickel 4-pentenyl chelate complex CpNi[$\eta^1$,$\eta^2$-$CH_2CH_2CH_2CH{=}CH_2$] (Cp = $C_5H_5$) isomerized at 70 °C in THF to form a mixture of $\pi$-allyl complexes CpNi($\eta^3$-$CH_3CHCHCHCH_3$) and CpNi($\eta^3$-$CH_2$-$CHCHCH_2CH_3$) (Scheme 7).[41] Similarly, the cationic platinum 4-pentenyl chelate complex [$(PMe_3)_2Pt(\eta^1,\eta^2$-$CH_2CMe_2CH_2$-$CH{=}CH_2)]^+$ $[BF_4]^-$ rearranged at −10 °C to form a mixture of the isomeric $\pi$-allyl complexes [$(PMe_3)_2Pt(\eta^3$-$CMe_2CH$-$CHMe)]^+$ $[BF_4]^-$ and [$(PMe_3)_2Pt(\eta^3$-$CH_2CMeCHMeCH_2CH_3)]^+$ $[BF_4]^-$.[42] The neutral rhodium 3-butenyl bis(phosphine) carbonyl chelate complex $(PPh_3)_2Rh(CO)[\eta^1,\eta^2$-$CH_2C(Ph)_2CH{=}CH_2]$ decomposed at 50 °C to form 1,1-diphenyl-1,3-butadiene in 44% yield.[43] Although treatment of the palladium norbornyl chloride

**Scheme 8**

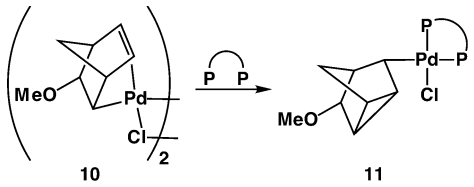


dimer **10** with dppe [dppe = bis(diphenylphosphino)ethane] led to rapid $\beta$-migratory insertion to form the palladium tricyclo-[2.2.1.$0^{0,0}$]heptyl complex **11**, the reactive alkyl olefin phosphine complex was not detected (Scheme 8).[44]

In two cases, $\beta$-migratory insertion of the olefin into the M−C bond of a 4-pentenyl chelate complex has been directly implicated through scrambling of deuterium atoms between the C(1) and C(3) carbon atoms of the pentenyl ligand. For example, Hallenbeck and Casey have reported that the yttrocene 4-pentenyl chelate complex $Cp^*_2Y[\eta^1,\eta^2$-$CD_2CH_2CH_2CH{=}CD_2]$ (**12**-1,1,5,5-$d_4$) ($Cp^* = C_5Me_5$) isomerized over 2 h at −78 °C to form a 1:1 mixture of **12**-1,1,5,5-$d_4$ and **12**-3,3,5,5-$d_4$ (Scheme 9).[45] Likewise, Flood has reported that thermolysis of the platinum 4-pentenyl chelate complex (dmpe)Pt[$\eta^1$,$\eta^2$-$CD_2CMe_2$-$CH_2CH{=}CH_2$] (**13**-1,1-$d_2$) [dmpe = bis(dimethylphosphino)-ethane] at 125 °C for 8 h formed a 1:1 mixture of **13**-1,1-$d_2$ and **13**-3,3-$d_2$.[46] However, in neither case was the cyclobutylmethyl intermediate observed and, for this reason, conversion of **5** to **6** represents the first direct observation of the $\beta$-migratory insertion of the coordinated olefin into the M−C bond of an alkyl olefin chelate complex. Furthermore, due to the substantial

(38) (a) Shultz, C. S.; Ledford, J.; DeSimone, J. M.; Brookhart, M. *J. Am. Chem. Soc.* **2000**, *122*, 6351. (b) Svejda, S. A.; Johnson, L. K.; Brookhart, M. *J. Am. Chem. Soc.* **1999**, *121*, 10634. (c) Brookhart, M.; Lincoln, D. M. *J. Am. Chem. Soc.* **1988**, *110*, 8719.
(39) (a) Brookhart, M.; Hauptman, E.; Lincoln, D. M. *J. Am. Chem. Soc.* **1992**, *114*, 10394. (b) Wang, L.; Flood, T. C. *J. Am. Chem. Soc.* **1992**, *114*, 3169.
(40) Lehmkuhl, H. *Pure Appl. Chem.* **1986**, *58*, 495 and references therein.
(41) Lehmkuhl, H.; Naydowski, C.; Benn, R.; Rufiñska, A.; Schroth, G.; Mynott, R.; Krüger, C. *Chem. Ber.* **1983**, *116*, 2447.
(42) Flood, T. C.; Statler, J. A. *Organometallics* **1984**, *3*, 1795.
(43) Jun, C.-H. *Organometallics* **1996**, *15*, 895.
(44) Coulson, D. R. *J. Am. Chem. Soc.* **1969**, *91*, 200.
(45) (a) Casey, C. P.; Hallenbeck, S. L.; Pollock, D. W.; Landis, C. R. *J. Am. Chem. Soc.* **1995**, *117*, 9770. (b) Casey, C. P.; Hallenbeck, S. L.; Wright, J. M.; Landis, C. R. *J. Am. Chem. Soc.* **1997**, *119*, 9681.
(46) (a) Flood, T. C.; Bitler, S. P. *J. Am. Chem. Soc.* **1984**, *106*, 6076. (b) Ermer, S. P.; Struck, G. E.; Bitler, S. P.; Richards, R.; Bau, R.; Flood, T. C. *Organometallics* **1993**, *12*, 2634.

*Scheme 9*

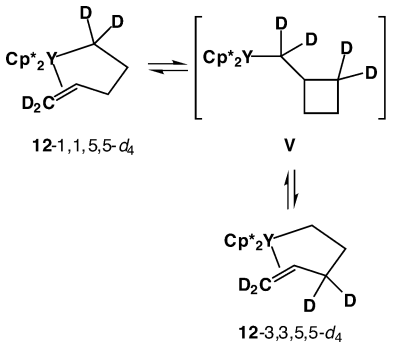


strain that accompanies cyclobutyl ring formation, the $\beta$-migratory insertion of **12** and **13** are not likely relevant to the $\beta$-migratory insertion processes that occur in synthetically relevant transition metal-catalyzed carbocyclization protocols.[2,47]

**Conversion of 5 to 6.** The zero-order dependence of the rate of conversion of **5** to **6** on nitrile concentration rules out a mechanism for the conversion of **5** to **6** initiated by attack of nitrile on **5** or a mechanism involving rapid and reversible conversion of **5** to **III** followed by rate-limiting ligand capture to form **6**. Rather, our kinetic data are in accord with a mechanism involving rate-limiting, irreversible conversion of **5** to **III** followed by rapid, exothermic ligand capture to form **6** (Scheme 6). DFT calculations indicate that olefin $\beta$-migratory insertion of ethylene into the Pd−C bond of **9** to form the palladium $\beta$-agostic butyl complex $[(H_2PCH{=}CHPH_2)Pd(CH_2CH_2CH_2CH_3)]^+$ is exothermic by ~8 kcal mol$^{-1}$ and, as noted above, complexation of ethylene to the $\beta$-agostic complex **8** is exothermic by ~12 kcal mol$^{-1}$. Because NCAr and ethylene possess comparable ligating ability with respect to cationic Pd(II) complexes,[16,24,36] we estimate that the conversion of **5** to **6** is also exothermic by ~20 kcal mol$^{-1}$.[48] From this value and from the enthalpy of activation for the conversion of **5** to **6** ($\Delta H^{\ddagger}$ = 13.5 kcal mol$^{-1}$), we estimate that the enthalpy of activation for the reverse reaction (**6** → **5**) is $\Delta H^{\ddagger} \approx 33$ kcal mol$^{-1}$, which clearly renders conversion of **5** to **6** irreversible under reaction conditions. Consistent with this conclusion, $\beta$-alkyl elimination has been observed only in the case of electrophilic d$^0$-metallocene complexes[49] and in strained cyclobutylmethyl[45,46] and cyclopropylmethyl complexes.[50,51] Because conversion of **5** to **6** is irreversible, and because the stereochemistry of alkyl olefin chelate complex **5** is likely determined thermodynamically (see above), conversion of **5** to **6** represents the stereochemistry-determining step in the palladium-catalyzed cyclization/hydrosilylation of **1**.

**Effect of the Chelate on Olefin $\beta$-Migratory Insertion.** Activation parameters for olefin $\beta$-migratory insertion have been determined for a number of nonchelated, cationic palladium alkyl olefin complexes.[15,16,25,26,30,31] Notable among these is the $\beta$-migratory insertion of the ethyl ethylene complex $[(phen)Pd(Et)(H_2C{=}CH_2)]^+ [BAr_4]^-$ (**14**) to form the *n*-butyl complex $[(phen)Pd(CH_2CH_2CH_2CH_3)]^+ [BAr_4]^-$ (**15**),[15] as complexes **5**, **6**, **14**, and **15** all possess the identical $(phen)Pd^+$ core. Activation parameters for conversion of **5** to **6** differ significantly from those for conversion of **14** to **15**, pointing to the influence of the hexenyl chelate on the energetics of olefin $\beta$-migratory insertion. For example, the entropy of activation for the conversion of **5** to **6** ($\Delta S^{\ddagger} = -15 \pm 2$ eu) is significantly more negative than is the entropy of activation for conversion of **14** to **15** ($\Delta S^{\ddagger} = -3.7 \pm 2$ eu); the latter value is typical for the olefin $\beta$-migratory insertion of nonchelated, late transition metal complexes.[39,52,53] Because the olefin ligand of **5** is oriented perpendicular to the coordination plane in the ground state but must lie parallel to the coordination plane in the transition state for $\beta$-migratory insertion,[54] the negative entropy of activation for the conversion of **5** to **6** indicates that the hexenyl chain adopts a more conformationally rigid orientation when the olefin is oriented in the coordination plane as opposed to perpendicular to the coordination plane. Although the olefin of **14** must also undergo 90° rotation prior to olefin $\beta$-migratory insertion, rotation of the ethylene ligand of **14** requires no reorganization elsewhere in the molecule.

Despite the less favorable $\Delta S^{\ddagger}$ for the conversion of **5** to **6** relative to $\Delta S^{\ddagger}$ for the conversion of **14** to **15**, the free energy of activation for the conversion of **5** to **6** ($\Delta G^{\ddagger} = 16.9 \pm 0.1$ kcal mol$^{-1}$) is 2.6 kcal mol$^{-1}$ lower than is the free energy of activation for the conversion of **14** to **15** ($\Delta G^{\ddagger} = 19.5 \pm 0.5$ kcal mol$^{-1}$) due to the significantly lower enthalpy of activation for the conversion of **5** to **6** ($\Delta H^{\ddagger} = 13.5 \pm 0.6$ kcal mol$^{-1}$) relative to the conversion of **14** to **15** ($\Delta H^{\ddagger} = 18.5 \pm 0.6$ kcal mol$^{-1}$).[55] This large difference in the enthalpy of activation ($\Delta\Delta H^{\ddagger} = 5$ kcal mol$^{-1}$) represents the most conspicuous difference in the activation parameters for the olefin $\beta$-migratory insertion of **5** and **14**. We attribute this large $\Delta\Delta H^{\ddagger}$ to ground-state destabilization of the alkyl olefin chelate complex **5**.[56] Assuming the preferred conformation of a transition metal alkyl olefin chelate complex mirrors that of a substituted cyclohexane ring, destabilization of **5** relative to **14** is suggested by the pseudoaxial orientation of the α-triethylsilylmethyl group of **5**. Presumably, unfavorable steric interactions within the hexenyl chain of **5** that result from the pseudoaxial orientation of the

(47) Flood also noted that "incorporation of substantial ring strain and conformational restrictions of the Pt−$CH_2$ group in the transition state [for the $\beta$-migratory insertion of **13**], especially the former, make the transition state potentially quite atypical."[46b]

(48) Although this analysis does not account for the likely destabilization of both **5** and **6** due to the presence of the hexenyl chelate and cyclopentyl ring, respectively, **5** and **6** are likely destabilized by a comparable amount relative to the corresponding acyclic derivatives. Destabilization of **5** by ~5 kcal mol$^{-1}$ relative to a nonchelated alkyl olefin complex is suggested by the lower $\Delta H^{\ddagger}$ for $\beta$-migratory insertion of **5** relative to that for unchelated derivative **14** ($\Delta\Delta H^{\ddagger} = 5$ kcal mol$^{-1}$) and by the pseudoaxial orientation of the α-triethylsilyl group of **5** in solution. Similarly, because there is approximately 6.5 kcal mol$^{-1}$ of strain energy associated with formation of a cyclopentyl ring, cyclopentylmethyl complex **6** is likely destabilized by ~6 kcal mol$^{-1}$ relative to the corresponding acyclic alkyl complex.

(49) (a) Watson, P. L. *J. Am. Chem. Soc*. **1982**, *104*, 6472. (b) Horton, A. D. *Organometallics* **1996**, *15*, 2675. (c) Guo, Z.; Swenson, D. C.; Jordan, R. F. *Organometallics* **1994**, *13*, 1424. (d) Hajela, S.; Bercaw, J. E.; *Organometallics* **1994**, *13*, 1147.

(50) Wang, X.; Stankovich, S. Z.; Widenhoefer, R. A. *Organometallics* **2002**, *21*, 901.

(51) In one notable exception, thermolysis of $[(dmpe)Pd(PMe_3)CH_2CMe_2Ph]^+ [BAr_4]^-$ [dmpe = $Me_2PCH_2CH_2PMe_2$; Ar = 3,5-$C_6H_3(CF_3)_2$] at 60 °C for 24 h led to $\beta$-phenyl elimination to form $[(dmpe)Pd(PMe_3)Ph]^+ [BAr_4]^-$: Cámpora, J.; Gutiérrez-Puebla, E.; López, J. A.; Monge, A.; Palma, P.; del Río, D.; Carmona, E. *Angew. Chem., Int. Ed.* **2001**, *40*, 3641.

(52) (a) Doherty, N. M.; Bercaw, J. E. *J. Am. Chem. Soc.* **1985**, *107*, 2670. (b) Berger, B. J. Santarsiero, B. D.; Trimmer, M. S. Bercaw, J. E. *J. Am. Chem. Soc.* **1988**, *110*, 3134.

(53) Although the entropy of activation for the reversible $\beta$-migratory insertion of the platinum 4-pentenyl chelate complex **13**-1,1-$d_2$ was near zero ($\Delta S^{\ddagger} = -0.5 \pm 1.6$ eu), $^1H-^1H$ NOESY analysis of **13**-1,1-$d_2$ was consistent with orientation of the olefin in or near the coordination plane, and for this reason, no significant olefin rotation or reorganization of the pentenyl chain was required for olefin $\beta$-migratory insertion.[46b]

(54) (a) Thorn, D. L.; Hoffmann, R. *J. Am. Chem. Soc*. **1978**, *100*, 2079. (b) Collman, J. P.; Hegedus, L. S.; Norton, J. R.; Finke, R. G. *Principles and Applications of Organotransition Metal Chemistry*; University Science Books: Mill Valley, CA, 1987.

α-triethylsilylmethyl group are less severe than is the steric interaction between the α-triethylsilylmethyl group and the phenanthroline ligand when the former adopts a pseudoequatorial orientation. Ground-state destabilization has been previously invoked to rationalize the decreasing $\Delta G^{\ddagger}$ for $\beta$-migratory insertion of propylene into the Pd−$CH_3$ bond of the palladium diimine complexes {[ArN═C(Me)C(Me)═NAr]Pd(Me)$CH_2$═CHMe}$^+$ with the increasing steric bulk of the diimine ligand.[30]

We considered two mechanisms by which the ground-state destabilization of **5** could decrease $\Delta H^{\ddagger}$ for the conversion of **5** to **6** relative to that of **14** to **15**. The in-plane rotamer of cationic palladium(II) phenanthroline olefin complexes is ∼10 kcal mol$^{-1}$ less stable than is the perpendicular rotamer;[14−16] calculations attribute destabilization of the in-plane rotamer to unfavorable steric interaction of the olefin ligand with the cis ligands.[57] Because it appears likely that the energy barrier for olefin rotation contributes significantly to the energy barrier for olefin $\beta$-migratory insertion,[54] destabilization of the perpendicular rotamer of **5** relative to the in-plane rotamer due to strain within the hexenyl chain would lead to lower $\Delta H^{\ddagger}$ for conversion of **5** to **6** relative to the conversion of **14** to **15**. Alternatively, DFT calculations for the $\beta$-migratory insertion of ethylene into the Pd−$CH_3$ bond of [(HN═CHCH═NH)Pd(Me)($H_2C$═$CH_2$)]$^+$ (**16**) to form [(HN═CHCH═NH)Pd($CH_2$-$CH_2CH_3$)]$^+$ (**17**) indicate that the $CH_3$−Pd−ethylene$_{(centroid)}$ angle decreases from 95° in the in-plane rotamer of **16** to 75° in the transition state for conversion of **16** to **17**.[58] Therefore, compression of the C−Pd−olefin$_{(centroid)}$ angle of **5** due to strain within the hexenyl chain could increase the extent of C−C bond formation in the transition state for the conversion of **5** to **6** relative to the transition state for the conversion of **14** to **15**, leading to a lower $\Delta H^{\ddagger}$ for the conversion of **5** to **6** relative to the conversion of **14** to **15**.

***Scheme 10***

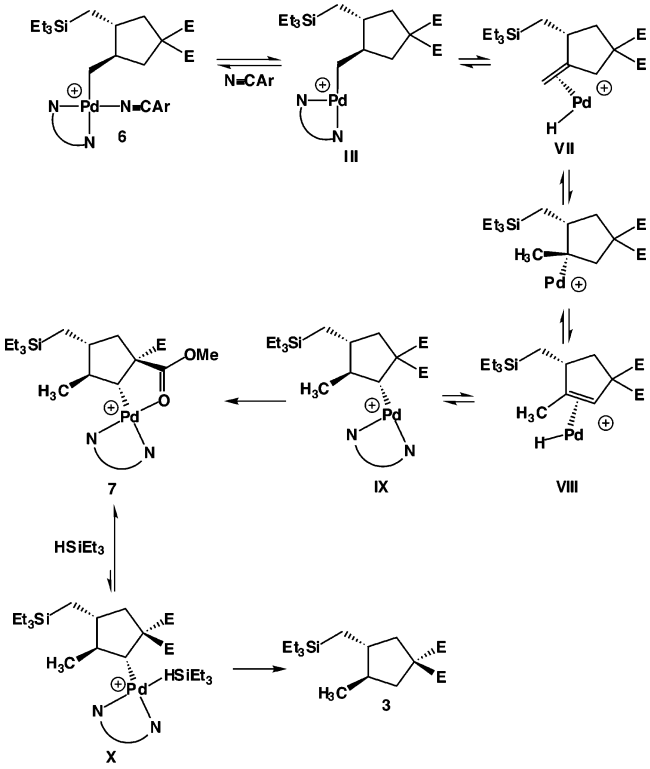


**Formation of Carbonyl Chelate Complex 7.** In the absence of silane, palladium cyclopentylmethyl complex **6** rearranges within 2 h at −9 °C to form the carbonyl chelate complex **7** with retention of stereochemistry (Scheme 2). Stereoselective conversion of **6** to **7** likely occurs via iterative $\beta$-hydride elimination/addition to form the palladium cyclopentyl intermediate **IX** without displacement of the olefin ligand from intermediates **VII** and **VIII**, followed by highly exoergonic complexation of the pendant carbonyl group to form **7** (Scheme 10). An analogous mechanism was proposed for formation of carbonyl chelate complex **7a** from stoichiometric reaction of **1** with **2c**.[17] Because both the formation and silylation of **7** are much slower than is the silylation of **6** under catalytic conditions (see below), we can conclusively rule out formation of **7** in the palladium-catalyzed cyclization/hydrosilylation of **1**.

**Silylation of Palladium Alkyl Complexes**. The first-order dependence of the rate of silylation of **7** on silane concentration rules out a mechanism for the silylation of **7** initiated by rate-limiting dissociation of the chelated carbonyl group. Furthermore, the much lower rate for the silylation of **7**, which possesses a tightly coordinated carbonyl chelate ligand, relative to the silylation of **6**, which possesses a labile NCAr ligand, argues against mechanisms for the silylation of **7** involving Pd−C bond cleavage without prior silane coordination or Pd−C bond cleavage from a five-coordinate palladium silane complex. Rather, our data are in accord with a mechanism for the conversion of **7** to **3** involving associative displacement of the carbonyl ligand of **7** with silane to form the four-coordinate palladium silane intermediate **X** followed by Pd−C bond cleavage to form **3**, perhaps via $\sigma$-bond metathesis (Scheme 10).[59]

(55) The free energy of activation for the $\beta$-migratory insertion of propene into the Pd−$CH_3$ bond of the cationic palladium propylene complex [(N−N)Pd(Me)$CH_2$═CHMe]$^+$ [N−N = ArN═C(Me)C(Me)═NAr, Ar = 2,6-$C_6H_3$-*i*-$Pr_2$] was only 0.5 kcal mol$^{-1}$ higher than was $\Delta G^{\ddagger}$ for the insertion of ethylene into the Pd−$CH_3$ bond of the corresponding palladium ethylene complex [(N−N)Pd(Me)$CH_2$═$CH_2$]$^+$.[25] For this reason, it appears unlikely that the lower $\Delta G^{\ddagger}$ and $\Delta H^{\ddagger}$ for olefin $\beta$-migratory insertion for **5** relative to that for **14** is due to the insertion of an α-olefin in the case of **5** and ethylene in the case of **14**. Furthermore, $\Delta G^{\ddagger}$ for $\beta$-migratory insertion of ethylene into the Pd−$CH_3$ bond of [(phen)Pd($CH_3$)($H_2C$═$CH_2$)]$^+$ [$BAr_4$]$^-$ was ∼1 kcal mol$^{-1}$ lower than was $\beta$-migratory insertion of ethylene into the Pd−$CH_2CH_3$ bond of **14**.[15,16] This comparison suggests that $\Delta G^{\ddagger}$ for olefin $\beta$-migratory insertion increases with increasing substitution of the palladium $\sigma$-bound carbon atom. For this reason, it appears highly unlikely that the lower $\Delta G^{\ddagger}$ for the conversion of **5** to **6** relative to the conversion of **14** to **15** is due to migration of a Pd-secondary alkyl group in the case of **5** and a palladium-primary alkyl group in the case of **14**.

(56) Enthalpic destabilization of **5** relative to **14** is not inconsistent with the failure to generate detectable amounts of the nonchelated palladium hexenyl complex **5-L** from reaction of **5** with **1** or NCAr (Scheme 3). An entropy of reaction for the conversion of **5** to **5-L** of $\Delta S \approx -30$ eu can be estimated from the values determined for displacement of the six-membered carbonyl chelate from the cationic palladium complex [(phen)Pd[$CH_2$-$CH_2CH_2$COOMe]$^+$ [$BAr_4$]$^-$ with ethylene and similar ligands ($\Delta S = -27$ to $-34$ eu).[16] Because NCAr and an α-olefin are of comparable ligating ability with respect to Pd(II),[36] the enthalpy for the conversion of **5** to **5-L** would be $\Delta H \approx 0$ if there were no significant destabilization of **5**. However, if we attribute the 5 kcal mol$^{-1}$ decrease in $\Delta H^{\ddagger}$ for $\beta$-migratory insertion of **5** relative to that for **14** solely to ground-state destabilization of **5**, the enthalpy of reaction for the conversion of **5** to **5-L** would be $\Delta H \approx -5$ kcal mol$^{-1}$. From these values ($\Delta H \approx -5$ kcal mol$^{-1}$, $\Delta S \approx -30$ eu) we estimate a free energy of reaction for the conversion of **5** to **5-L** of $\Delta G \approx$ 2 kcal mol$^{-1}$, which corresponds to an equilibrium constant of $K_{eq} \approx 8 \times 10^{-3}$ at −62 °C. Therefore, **5-L** should constitute less than 0.1% of a mixture of **5** (42 mM), **1** (42 mM), and NCAr (42 mM) at −62 °C and, therefore, **5-L** should be undetectable by $^1$H NMR analysis under these conditions.

(57) Hay, P. J. *J. Am. Chem. Soc*. **1981**, *103*, 1390.

(58) Svensson, M.; Matsubara, T.; Morokuma, K. *Organometallics* **1996**, *15*, 5568.

(59) Alternatively, Pd−C bond cleavage could occur via an oxidative addition/reductive elimination sequence.

*Scheme 11*

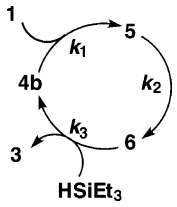


All available evidence regarding the silylation of **6** points to an associative mechanism involving palladium silane intermediate **IV** (Scheme 6). The strong inhibition of the rate of the silylation of **6** by $CD_3CN$ and the much higher rate of the silylation of **6** relative to the silylation of **7** argues against mechanisms for the silylation of **6** involving Pd−C bond cleavage without prior silane coordination or Pd−C bond cleavage from a five-coordinate palladium silane complex. Although the first-order dependence of the rate of the silylation of **6** on silane concentration was not directly established, silane competition experiments support this contention. Provided that scrambling of the silyl group of **4b′** with free silane is slow relative to irreversible conversion of **4b′** to **5′**,[60,61] the ratio of silylated carbocycles formed in the catalytic cyclization/hydrosilylation of **1** with an excess 1:1 mixture of two different silanes corresponds to the relative rate at which the two silanes react with palladium cyclopentylmethyl complex **6′**. Therefore, silane competition experiments establish that the rate of silylation of **6′** increases with both the decreasing steric bulk and increasing electron density of the silane. Both of these observations are consistent with a mechanism for silylation involving direct attack of the silane on the palladium atom of **6′**.[62]

**Kinetics of Catalytic Cyclization/Hydrosilylation**. The kinetics of the catalytic cyclization/hydrosilylation of **1** and $HSiEt_3$ were interpreted in the context of the simplified mechanism depicted in Scheme 11, which was constructed on the basis of the following assumptions: (1) conversion of **4b** to **5**, **5** to **6**, and **6** to **4b** is irreversible, (2) the total palladium concentration equals the initial concentration of **2b** ($[Pd]_{tot} = [\mathbf{2b}]_0$), (3) conversion of **2b** to **4b** is fast relative to catalyst turnover,[63] and (4) the rate of silylation of **6** depends linearly on silane concentration (see above). Steady-state treatment of intermediates **4b** and **6** produced the three-term rate law depicted in eq 1, which simplifies to the two-term rate law depicted in eq 2 when the conversion of **4** to **5** is much faster than is the conversion of **5** to **6**, and to the single-term rate law depicted in eq 3, when both the conversion of **4** to **5** and the silylation of **6** are fast relative to the conversion of **5** to **6**.[64]

$$\text{rate} = \frac{k_2[\text{Pd}]_{tot}}{1 + \frac{k_2}{k_1[1]} + \frac{k_2}{k_3[\text{HSiEt}_3]}} \qquad \text{eq 1}$$

$$k_1[1] >> k_2: \quad \text{rate} = \frac{k_2 k_3[\text{HSiEt}_3][\text{Pd}]_{tot}}{k_3[\text{HSiEt}_3] + k_2} \qquad \text{eq 2}$$

$$k_1[1] >> k_2 \text{ and } k_3[\text{HSiEt}_3] >> k_2: \quad \text{rate} = k_2[\text{Pd}]_{tot} \qquad \text{eq 3}$$

All of our experimental observations point to turnover-limiting conversion of alkyl olefin chelate complex **5** to cyclopentylmethyl complex **6** in the catalytic conversion of **1** to **3** at high silane concentration ($[HSiEt_3]_0 = 0.16$ M). For example, the empirical rate law for the catalytic cyclization/hydrosilylation of **1** and $HSiEt_3$ at high silane concentration (rate $= k_{sat}[\mathbf{2b}]_0$) is of the same form as the derived rate law depicted in eq 3 (rate $= k_2[Pd]_{tot}$). Likewise, the activation parameters for the catalytic conversion of **1** to **3** at high silane concentration ($\Delta G^{\ddagger}_{232K} = 16.8 \pm 0.1$ kcal mol$^{-1}$; $\Delta H^{\ddagger} = 13 \pm 1$ kcal mol$^{-1}$; $\Delta S^{\ddagger} = -15 \pm 3$ eu) do not differ significantly from those determined independently for the conversion of **5** to **6** ($\Delta G^{\ddagger}_{232\,K} = 16.9 \pm 0.1$ kcal mol$^{-1}$; $\Delta H^{\ddagger} = 13.5 \pm 0.6$ kcal mol$^{-1}$; $\Delta S^{\ddagger} = -15 \pm 2$ eu). Furthermore, alkyl olefin chelate complex **5** was the only palladium species detected during catalytic cyclization/hydrosilylation of **1** at high silane concentration, which establishes **5** as the catalyst resting state under these conditions.

The pronounced positive curvature of the concentration versus time plots for the catalytic cyclization/hydrosilylation of **1** at lower silane concentration ($[HSiEt_3]_0 = 90$ mM, Figure 6) indicates that under these conditions, the rate of silylation of cyclopentylmethyl complex **6** is both comparable to the rate of conversion of **5** to **6** and is dependent on silane concentration. Iterative fitting of two sets of concentration versus time data for the catalytic cyclization/hydrosilylation of **1** at low silane concentration ($[HSiEt_3]_0 = 90$ mM) to the rate law depicted in eq 2 provided a best fit with $k_2 = 7.6 \pm 0.2 \times 10^{-4}$ s$^{-1}$ and $k_3 = 0.12 \pm 0.03$ M$^{-1}$ s$^{-1}$. Noteworthy is that the value for $k_2$ extracted from this analysis is in good agreement with the value obtained under saturation conditions ($k_{sat} = k_2 = 7.74 \pm 0.06 \times 10^{-4}$ s$^{-1}$). Furthermore, because silylation of **6** is likely

(60) The designators **4b′**, **5′**, and **6′** refer to the palladium silyl, alkyl olefin chelate, and cyclopentylmethyl derivatives, respectively, with an undefined silyl group $-SiMe_2R$ (R = Et, *n*-octyl, $OSiMe_3$, Ph, 4-$C_6H_4NMe_2$, 4-$C_6H_4$-OMe, 4-$C_6H_4F$, or 4-$C_6H_4CF_3$) generated in the catalytic silane competition experiments.

(61) Brookhart has shown that reaction of palladium silyl olefin complex $[(phen)Pd(SiEt_3)(CH_2{=}CH\textit{t}\text{-Bu})]^+$ $[BAr_4]^-$ [Ar = 3,5-$C_6H_3(CF_3)_2$] (**4e**) with $HSiPh_3$ formed (3,3-dimethylbutyl)triethylsilane to the exclusion of (3,3-dimethylbutyl)triphenylsilane,[14] which indicates that olefin insertion/silylation of **4e** is much faster than is silyl exchange. Because NCAr and an olefin of **1** are of comparable ligating ability with respect to cationic Pd(II) complexes,[36] this result strongly suggests that **4b** does not undergo silyl exchange prior to conversion to **5**.

(62) Silane competition experiments are in accord with either rate-limiting conversion of **6** to **IV** followed by rapid conversion of **IV** to **3**, or rapid and reversible conversion of **6** to **IV** followed by rate-limiting conversion of **IV** to **3**. The transition states for both the conversion of **6** to **IV** (**6**$^{\ddagger}$) and **VI** to **4b** (**IV**$^{\ddagger}$) should possess a greater degree of covalent Pd−Si bond character than do **6** and **IV**, respectively. Likewise, the Pd−Si bond distance should decrease upon conversion of both **6** to **6**$^{\ddagger}$ and **IV** to **IV**$^{\ddagger}$. Therefore, both **6**$^{\ddagger}$ and **IV**$^{\ddagger}$ should be destabilized by the decreasing electron density and increasing steric bulk of the silane.

(63) Available evidence supports each of these assumptions. The failure of **1**-2,6-$d_2$ to exchange with the 5-hexenyl group of **5** establishes irreversible conversion of **4b** to **5**, analysis of DFT data supports the irreversible conversion of **5** to **6**,[37] and Brookhart has established the irreversible silylation of a Pd−C bond with a hydrosilane.[14] Visual inspection of catalytically active mixtures of **1**, **2b**, and $HSiEt_3$ revealed no darkening of the solution prior to complete consumption of **1**, which argues against catalyst decomposition during cyclization/hydrosilylation. The much faster conversion of **2b** and $HSiEt_3$ to **4b** (5 min at −80 °C) relative to the conversion of **5** to **6** ($t_{1/2} = 22$ min at −41 °C) ensures rapid activation of precatalyst **2b** relative to catalyst turnover.

(64) Although the mechanism for cyclization/hydrosilylation depicted in Scheme 6 likely involves nitrile inhibition of both the conversion of **4b** to **5** and the conversion of **6** to **4b**, both these transformations are fast relative to the conversion of **5** to **6** at high silane concentration ($[HSiEt_3]_0 = 0.16$M). Although conversion of **6** to **4b** becomes kinetically relevant at low silane concentration, nitrile concentration was invariant ([NCAr] = 42 mM) throughout complete conversion of **1** to **3** and between multiple experiments. Therefore, $k_3$ corresponds to a macroscopic rate constant for the conversion of **6** to **4b** for the specific case where [NCAr] = 42 mM.

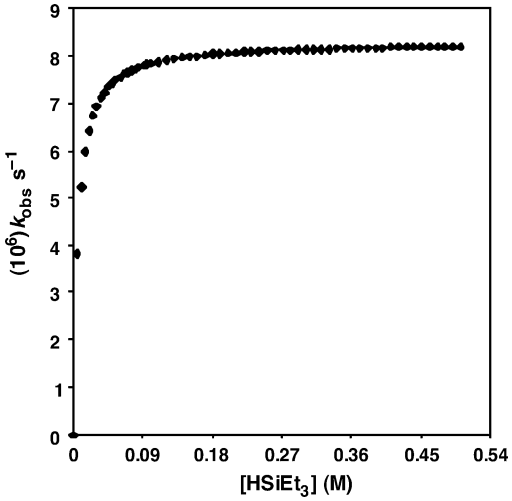


***Figure 9.*** Theoretical plot of $k_{obs}$ versus [$HSiEt_3$] for the catalytic cyclization/hydrosilylation of **1** and $HSiEt_3$ calculated from eq 2 where [**1**] = 85 mM, $[Pd]_{tot}$ = 12 mM, and [NCAr] = 42 mM, $k_2 = 7.6 \times 10^{-4}$ s$^{-1}$, and $k_3 = 0.12$ M$^{-1}$ s$^{-1}$.

inhibited by nitrile, the value for $k_3$ extracted from this analysis ([NCAr] = 42 mM) is in accord with the rate constant estimated for the silylation of **6** under stoichiometric conditions ([NCAr] $\approx$ 0 mM, $k \geq 0.19$ M$^{-1}$ s$^{-1}$).[27]

To better visualize the dependence of the rate of catalytic cyclization/hydrosilylation on silane concentration, a hypothetical plot of $k_{obs}$ versus [$HSiEt_3$] for the catalytic cyclization/hydrosilylation of **1** and $HSiEt_3$ was generated by solving eq 2 for $k_{obs}$ ($k_{obs}$ = rate/[**1**]) as a function of [$HSiEt_3$] in 0.01 M increments from 0 to 0.50 M, where [**1**] = 85 mM, $[Pd]_{tot}$ = 12 mM, and [NCAr] = 42 mM, $k_2 = 7.6 \times 10^{-4}$ s$^{-1}$, and $k_3 = 0.12$ M$^{-1}$ s$^{-1}$ (Figure 9). This theoretical plot indicates that the rate of catalytic cyclization/hydrosilylation should decrease less than 3% as the silane concentration decreases from 0.16 to 0.080 M, which is in accord with the observed linearity of the concentration versus time plots for catalytic cyclization/hydrosilylation at high silane concentration ($[HSiEt_3]_0 = 0.16$ M) through 90% conversion (Figure 6). Likewise, the theoretical plot predicts that the rate of catalytic cyclization/hydrosilylation should decrease $\sim$50% as the silane concentration decreases from 90 to 5 mM, which is in accord with the pronounced positive curvature of the concentration versus time plots for catalytic cyclization/hydrosilylation at low silane concentration ($[HSiEt_3]_0 = 90$ mM) through 95% conversion (Figure 6).

## Conclusions

All of our observations support the mechanism for the cyclization/hydrosilylation of **1** and $HSiEt_3$ catalyzed by **2b** depicted in Scheme 6. Rapid and reversible complexation of one of the double bonds of **1** with palladium silyl intermediate **4b** would form the unobserved palladium olefin complex **I**. $\beta$-Migratory insertion of the olefin into the Pd−Si bond of **I** to form the palladium 5-hexenyl complex **II**, followed by rapid, irreversible complexation of the pendant olefin would form alkyl olefin chelate complex **5**. Although not detected, associative displacement of the chelated olefin of **5** by exogenous ligand is likely and, for this reason, the diastereoselective formation of **5** is under thermodynamic control. $\beta$-Migratory insertion of the pendant olefin into the Pd−C bond of **5** to form the palladium cyclopentylmethyl complex **III** followed by rapid,

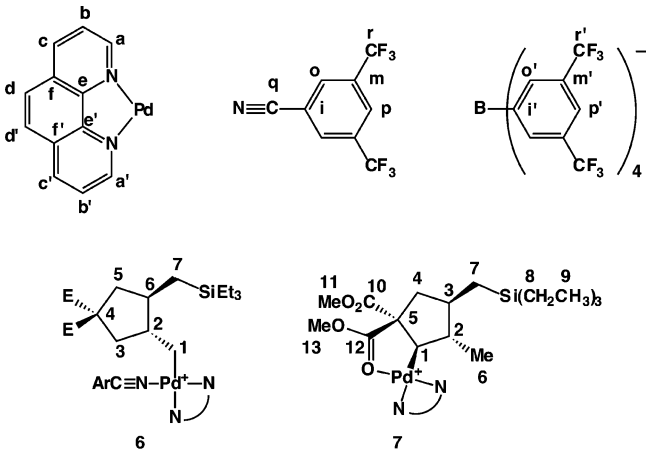


***Figure 10.*** Atom-labeling schemes for phenanthroline, NCAr, $BAr_4^-$, **6**, and **7**.

exothermic ligand capture with NCAr forms **6**. Conversion of **5** to **6** is likely irreversible and is therefore the stereochemistry-determining step in catalytic cyclization/hydrosilylation. The enthalpy of activation for $\beta$-migratory insertion of the olefin into the Pd−C bond of **5** is 5 kcal mol$^{-1}$ lower than is $\Delta H^{\ddagger}$ for $\beta$-migratory insertion of the olefin into the Pd−C bond of the analogous nonchelated alkyl olefin complex **14**. We attribute this large $\Delta\Delta H^{\ddagger}$ to ground-state destabilization of **5** relative to **14**. Associative silylation of **6** via palladium−silane intermediate **IV** releases carbocycle **3** and regenerates palladium silyl complex **4b**. Under catalytic conditions, the second-order rate constant for the silylation of **6** ($k_3 = 0.12 \pm 0.03$ M$^{-1}$ s$^{-1}$) is $\sim$160 times greater than is the first-order rate constant for conversion of **5** to **6** ($k_2 = 7.6 \pm 0.2 \times 10^{-4}$ s$^{-1}$), and both of these processes are slow relative to the conversion of **4b** to **5**. Therefore, at high silane concentration ([$HSiEt_3$] > 85 mM), silylation of **6** is fast relative to conversion of **5** to **6**, and the latter step alone determines the rate of catalytic cyclization/hydrosilylation. Conversely, at low silane concentration ([$HSiEt_3$] < 85 mM), the rate of silylation of **6** becomes competitive with the rate of conversion of **5** to **6** and the rate of catalytic cyclization/hydrosilylation depends on silane concentration. Although cyclopentylmethyl complex **6** rearranges to oxo chelate complex **7** in the absence of silane, neither the conversion of **6** to **7** nor the silylation of **7** with $HSiEt_3$ to form **3** is fast enough to compete with the silylation of **6** under catalytic conditions.

## Experimental Section

**General Methods.** Low-temperature NMR spectra were recorded at 500 MHz for $^1$H and 125 MHz for $^{13}$C, except where noted; room-temperature NMR spectra were recorded at 400 MHz for $^1$H and 100 MHz for $^{13}$C, except where noted. NMR Probe temperatures were measured with a methanol thermometer and were maintained to within $\pm$ 0.5 °C. Atom-labeling schemes for phenanthroline, NCAr, $BAr_4^-$, **6**, and **7** are shown in Figure 10. $^1$H NMR yields for the conversion of **4b** to **5**, **5** to **6**, and **6** to **7** were determined employing a 10 s delay between pulses. Unless noted otherwise, error limits for rate constants refer to the standard deviation of the slope of the respective kinetic plot or to the standard deviation of the average of multiple experiments. The volumes of low-temperature NMR solutions were calculated from the room-temperature volume and the temperature dependence of the density of $CH_2Cl_2$; volumes given refer to the volume at the specified reaction temperature. Elemental analysis was performed by Complete Analysis Laboratories, Inc. (Parsippany, NJ).

**[(phen)Pd(SiEt$_3$)(NCAr)]$^+$ [BAr$_4$]$^-$ (4b).** HSiEt$_3$ (2.62 mg, 22.5 $\mu$mol) was added via syringe to an NMR tube containing a solution of [(phen)Pd(Me)(NCAr)]$^+$ [BAr$_4$]$^-$ (**2b**) (31.6 mg, 22.5 $\mu$mol) in $CD_2Cl_2$ (0.54 mL) at −78 °C. The tube was shaken briefly and placed into the probe of an NMR spectrometer pre-cooled at −81 °C. Reaction progress was determined by measuring the disappearance of the Pd−$CH_3$ resonance of **2b** ($\delta$ 1.26) relative to the para phenyl protons of the [BAr$_4$]$^-$ counterion ($\delta$ 7.46) in the $^1$H NMR spectrum. After 5 min, **2b** was completely consumed to form **4b** in 101 ± 10% yield. Complex **4b** was thermally sensitive and characterized in solution at −81 °C by $^1$H NMR spectroscopy. $^1$H NMR ($CD_2Cl_2$, −81 °C): $\delta$ 9.02 (d, $J$ = 4.9 Hz, 1 H, $H_{phen}$), 8.83 (d, $J$ = 4.5 Hz, 1 H, $H_{phen}$), 8.55 (d, $J$ = 8.2 Hz, 1 H, $H_{phen}$), 8.43 (d, $J$ = 8.3 Hz, 1 H, $H_{phen}$), 8.39 (s, 2 H, $H_o$), 8.36 (s, 1 H, $H_p$), 7.93 (m, 3 H, $H_{phen}$), 7.78 (dd, $J$ = 4.8, 8.0 Hz, 1 H, $H_b$), 7.73 (s, 8 H, $H_{o'}$), 7.46 (s, 4 H, $H_{p'}$), 1.06 (t, $J$ = 7.5 Hz, 9 H, SiCH$_2$C*H*$_3$), 0.97 (q, $J$ = 7.5 Hz, 6 H, SiC*H*$_2$CH$_3$).

**{(phen)Pd[$\eta^1$,$\eta^2$-CH(CH$_2$SiEt$_3$)CH$_2$C(CO$_2$Me)$_2$CH$_2$CH=CH$_2$]}$^+$ [BAr$_4$]$^-$ (5).** Dimethyl diallylmalonate (**1**) (4.7 $\mu$L, 0.023 mmol) was added via syringe to an NMR tube containing a solution of [(phen)Pd(SiEt$_3$)(NCAr)]$^+$ [BAr$_4$]$^-$ (**4b**) (0.023 mmol) in $CD_2Cl_2$ (0.55 mL) at −78° C. The tube was shaken briefly and placed in the probe of an NMR spectrometer pre-cooled at −81 °C. The probe was warmed at −62 °C and the solution was analyzed periodically by $^1$H NMR spectroscopy. Reaction progress was determined by integrating the carbomethoxy resonances of **5** ($\delta$ 3.68 and 3.43) relative to that of the para phenyl proton of the BAr$_4^-$ counterion ($\delta$ 7.49). After 20 min, **4b** was completely consumed to form **5** as the exclusive product in 84% ± 10% yield as a single diastereomer characterized by $^1$H NMR spectroscopy. Complex **5** was thermally sensitive and was characterized in solution by $^1$H NMR spectroscopy at −62 °C. Assignment of the proton resonances and $J_{HH}$ coupling constants of **5** was aided by $^1$H−$^1$H COSY analysis and by $^1$H NMR analysis of the deuterated isotopomers {(phen)Pd[$\eta^1$,$\eta^2$-CD(CH$_2$SiEt$_3$)CH$_2$C(CO$_2$Me)$_2$CH$_2$CD=CH$_2$]}$^+$ [BAr$_4$]$^-$ (**5**-$d_2$) and {(phen)Pd[$\eta^1$,$\eta^2$-CH(CH$_2$SiEt$_3$)CD$_2$C(CO$_2$Me)$_2$CD$_2$CH=CH$_2$]}$^+$ [BAr$_4$]$^-$ (**5**-$d_4$) (see Supporting Information).

**For 5:** $^1$H NMR ($CD_2Cl_2$, −62 °C): $\delta$ 8.71 (d, $J$ = 4.4 Hz, 1 H, $H_a$), 8.61 (d, $J$ = 8.1 Hz, 1 H, $H_c$), 8.48 (dd, $J$ = 1.2, 8.2 Hz, 1 H, $H_c$), 8.35 (dd, $J$ = 1.2, 4.9 Hz, 1 H, $H_a$), 8.16 (s, 2 H, $H_o$), 8.14 (s, 1 H, $H_p$), 8.05 (dd, $J$ = 5.2, 8.0 Hz, 1 H, $H_b$), 7.96 (s, 2 H, $H_d$), 7.87 (dd, $J$ = 4.9, 8.1 Hz, 1 H, $H_b$), 7.74 (s, 8 H, $H_{o'}$), 7.49 (s, 4 H, $H_{p'}$), 6.41 (dddd, $J$ = 4.3, 8.2, 9.0, 16.1 Hz, 1 H, −C*H*=CH$_2$), 5.44 (d, $J$ = 9.0 Hz, 1 H, −CH=C*H*$_2$), 4.22 (d, $J$ = 16.1 Hz, 1 H, −CH=C*H*$_2$), 3.68 (s, 3 H, CO$_2$*Me*), 3.43 (s, 3 H, CO$_2$*Me*), 3.02 (dd, $J$ = 8.2, 12.7 Hz, 1 H, −C*H*$_2$-CH=CH$_2$), 2.66 (m, 1 H, Pd−C*H*), 2.22 (dd, $J$ = 4.0, 12.6 Hz, 1 H, −C*H*$_2$CH=CH$_2$), 1.74, 1.70 [ABX, $J_{AB}$ = 15.6 Hz, $J_{AX}$ = 10.9 Hz, $J_{BX}$ = 5.4 Hz, 2 H, Pd−CH(CH$_2$SiEt$_3$)C*H*$_2$], 1.23 [dd, $J$ = 2.6, 13.3 Hz, 1 H, Pd−CH(C*H*$_2$SiEt$_3$)CH$_2$], 1.11 [t, $J$ = 13.3 Hz, 1 H, Pd−CH-(C*H*$_2$SiEt$_3$)], 0.94 (t, $J$ = 7.9 Hz, 9 H, SiCH$_2$C*H*$_3$), 0.64 (q, $J$ = 7.9 Hz, 6 H, SiC*H*$_2$CH$_3$).

**{(phen)Pd[$\eta^1$,$\eta^2$-CH(CH$_2$SiEt$_3$)CH$_2$$^{13}$C($^{13}$CO$_2$Et)$_2$CH$_2$CH=CH$_2$]}$^+$ [BAr$_4$]$^-$ (5a-$^{13}$C$_3$).** Reaction of diethyl diallylmalonate $^{13}$C labeled at each of the quaternary carbon atoms (**1a**-$^{13}$C$_3$, 4.7 $\mu$L, 0.023 mmol) and **4b** (0.023 mmol) in $CD_2Cl_2$ (0.56 mL) at −62° C, employing a procedure analogous to that used in the synthesis of **5**, gave **5a**-$^{13}$C$_3$ as the exclusive product by $^1$H NMR analysis. $^{13}$C{$^1$H} NMR ($CD_2Cl_2$, −62 °C, labeled carbon atoms only): $\delta$ 172.6 (dd, $J$ = 2.3, 55.3 Hz), 172.5 (d, $J$ = 58.4 Hz), 65.5 (dd, $J$ = 55.2, 58.4 Hz).

**{(phen)Pd[$\eta^1$,$\eta^2$-$^{13}$CH($^{13}$CH$_2$SiEt$_3$)$^{13}$CH$_2$C(CO$_2$Me)$_2$$^{13}$CH$_2$$^{13}$CH=$^{13}$CH$_2$]}$^+$ [BAr$_4$]$^-$ (5-$^{13}$C$_6$).** Reaction of **1**-1,2,3,5,6,7-$^{13}$C$_6$ (4.2 $\mu$L, 0.021 mmol) and **4b** (0.022 mmol) in $CD_2Cl_2$ (0.56 mL) at −60 °C employing a procedure analogous to that used to synthesize **5** gave **5**-$^{13}$C$_6$ as the exclusive product by $^1$H NMR analysis. $^{13}$C{$^1$H} NMR ($CD_2Cl_2$, 75 MHz −60 °C, labeled carbon atoms only): $\delta$ 103.7 (dd, $J$ = 41, 47 Hz, −*C*H=CH$_2$), 87.5 (d, $J$ = 47 Hz, −CH=*C*H$_2$), 50.0 [dd, $J$ = 30, 36 Hz, Pd−*C*H(CH$_2$SiEt$_3$)CH$_2$], 39.2 [d, $J$ = 36 Hz, Pd−CH(CH$_2$SiEt$_3$)-*C*H$_2$], 32.5 (d, $J$ = 41 Hz, −*C*H$_2$CH=CH$_2$), 20.3 [d, $J$ = 30 Hz, Pd−CH(*C*H$_2$SiEt$_3$)CH$_2$].

**Exchange of 1-2,6-$d_2$ with 5.** Diene **1**-2,6-$d_2$ (5.88 $\mu$L, 29.2 mmol) was added via syringe to an NMR tube containing a solution of **5** (~25 mmol) in $CD_2Cl_2$ (0.58 mL) at −80 °C. The tube was shaken briefly and placed in the probe of an NMR spectrometer cooled at −80 °C. The sample was maintained at −80 °C for 1.5 h and then warmed at −60 °C for 30 min. At this time, $^1$H NMR analysis revealed approximately 5% conversion to **6** without formation of either free **1** or **5**-$d_2$.

***trans*-{(phen)Pd[CH$_2$CHCH$_2$C(CO$_2$Me)$_2$CH$_2$CHCH$_2$SiEt$_3$]-(NCAr)}$^+$ [BAr$_4$]$^-$ (6).** An NMR tube containing a solution **5** (39 mM) and NCAr (39 mM) in $CD_2Cl_2$ was warmed at −41 °C and monitored periodically by $^1$H NMR spectroscopy; reaction progress was determined by integrating the carbomethoxy resonances of **6** ($\delta$ 3.67 and 3.59) and **5** ($\delta$ 3.69 and 3.43) relative to the para phenyl resonances of the BAr$_4^-$ counterion ($\delta$ 7.51). After 2 h, **5** had been completely consumed to form **6** in 96 ± 10% yield by $^1$H NMR analysis. Complex **6** was thermally sensitive and was characterized in solution by $^1$H and $^{13}$C NMR spectroscopy at ≤−41 °C. Assignment of proton resonances and $J_{HH}$ coupling constants was aided by $^1$H COSY analysis and by $^1$H NMR analysis of the labeled derivatives *trans*-{(phen)Pd[CH$_2$CDCH$_2$C-(CO$_2$Me)$_2$CH$_2$CDCH$_2$SiEt$_3$](NCAr)}$^+$ [BAr$_4$]$^-$ (**6**-$d_2$) and *trans*-{(phen)Pd[CH$_2$CHCD$_2$C(CO$_2$Me)$_2$CD$_2$CHCH$_2$SiEt$_3$](NCAr)}$^+$ [BAr$_4$]$^-$ (**6**-$d_4$) (see Supporting Information).

**For 6:** $^1$H NMR ($CD_2Cl_2$, −41 °C): $\delta$ 8.86 (dd, $J$ = 1.0, 5.4 Hz, 1 H, $H_a$), 8.84 (dd, $J$ = 1.5, 4.9 Hz, 1 H, $H_a$), 8.65 (s, 2 H, $H_o$), 8.64 (dd, $J$ = 1.1, 8.6 Hz, 1 H, $H_c$), 8.55 (dd, $J$ = 1.5, 8.4 Hz, 1 H, $H_c$), 8.38 (s, 1 H, $H_p$), 8.02 (d, $J$ = 2.7 Hz, 2 H, $H_d$), 7.99 (dd, $J$ = 5.4, 8.2 Hz, 1 H, $H_b$), 7.86 (dd, $J$ = 4.8, 8.2 Hz, 1 H, $H_b$), 7.72 (s, 8 H, $H_{o'}$), 7.51 (s, 4 H, $H_{p'}$), 3.67 (s, 3 H, CO$_2$C*H*$_3$), 3.59 (s, 3 H, CO$_2$C*H*$_3$), 2.93 (dd, $J$ = 7.4, 13.5 Hz, 1 H, $H_3$), 2.62 (dd, $J$ = 6.3, 13.1 Hz, 1 H, $H_5$), 2.52 (dd, $J$ = 4.0, 7.7 Hz, 1 H, $H_1$), 2.18 (dd, $J$ = 10.4, 13.4 Hz, 1 H, $H_3$), 2.09 (dd, $J$ = 8.3, 10.8 Hz, 1 H, $H_1$), 1.80 (m, 1 H, $H_2$), 1.77 (dd, $J$ = 11.9, 12.9 Hz, 1 H, $H_5$), 1.67 (m, 1 H, $H_6$), 1.26 (dd, $J$ = 3.0, 13.4 Hz, 1 H, $H_7$), 0.92 (t, $J$ = 7.9 Hz, 9 H, −SiCH$_2$C*H*$_3$), 0.55 (q, $J$ = 7.9 Hz, 6 H, −SiC*H*$_2$CH$_3$), 0.46 (dd, $J$ = 11.9, 13.6 Hz, 1 H, $H_7$). $^{13}$C{$^1$H} NMR ($CD_2Cl_2$, −62 °C): $\delta$ 175.4 (*C*O$_2$CH$_3$), 175.2 (*C*O$_2$CH$_3$), 163.8 (q, $J_C11_B$ = 49.7 Hz, superimposed on a septet, $J_{C^{10}B}$ = 16.8 Hz, $C_i$), 159.4, 150.5, 149.6, 145.4, 142.4, 141.4 ($C_{phen}$), 136.6 ($C_{o'}$), 136.1 ($C_o$), 134.9 (q, $^2J_{CF}$ = 35.1 Hz, $C_m$), 132.6, 132.0 ($C_{phen}$), 131.3 ($C_p$), 130.6 (q, $^2J_{CF}$ = 31.4 Hz, $C_{m'}$), 129.9, 129.6, 127.9, 127.8 ($C_{phen}$), 126.4 (q, $^1J_{CF}$ = 273 Hz, $C_{r'}$), 124.1 (q, $^1J_{CF}$ = 274 Hz, $C_r$), 121.5, 113.8 ($C_i$ and $C_q$), 119.5 ($C_{p'}$), 59.2 ($C_4$), 55.3 (CO$_2$CH$_3$), 55.2 (CO$_2$CH$_3$), 53.6 ($C_2$), 45.2, 44.8, 43.9 ($C_3$, $C_5$, and $C_6$) 32.4 ($C_1$), 16.0 ($C_7$), 9.5 (SiCH$_2$CH$_3$), 5.2 (SiCH$_2$CH$_3$).

***trans*-{(phen)Pd[CH$_2$CHCH$_2$$^{13}$C($^{13}$CO$_2$Et)$_2$CH$_2$CHCH$_2$SiEt$_3$]-(NCAr)}$^+$ [BAr$_4$]$^-$ (6a-$^{13}$C$_3$).** Warming a solution of **5a**-$^{13}$C$_3$ (4.66 $\mu$L, 0.023 mmol) in $CD_2Cl_2$ (0.60 mL) at −41 °C for 2 h formed **6a**-$^{13}$C$_3$ as the exclusive product by $^1$H NMR analysis. $^{13}$C{$^1$H} NMR ($CD_2Cl_2$, −41 °C, labeled carbon atoms only): $\delta$ 175.4 (dd, $J$ = 1.4, 58.4 Hz, *C*O$_2$CH$_3$), 175.2 (dd, $J$ = 1.4, 58.4 Hz, *C*O$_2$CH$_3$), 59.2 (t, $J$ = 58.4 Hz, $C_4$).

***trans*-{(phen)Pd[$^{13}$CH$_2$$^{13}$CH$^{13}$CH$_2$C(CO$_2$Me)$_2$$^{13}$CH$_2$$^{13}$CH$^{13}$CH$_2$SiEt$_3$]-(NCAr)}$^+$ [BAr$_4$]$^-$ (6-$^{13}$C$_6$).** Warming a solution of **5**-$^{13}$C$_6$ (0.021 mmol) in $CD_2Cl_2$ (0.60 mL) at −40 °C for 2 h formed **6**-$^{13}$C$_6$ as the exclusive product by $^1$H NMR analysis. $^{13}$C{$^1$H} NMR ($CD_2Cl_2$, 75 MHz −40 °C, labeled carbon atoms only): $\delta$ [51.8 (q), 43.3 (q), $C_2$ and $C_6$)], [42.7 (d), 42.2 (d), 31.0 (d), $C_1$, $C_3$ and $C_5$], 14.8 (d, $C_7$); all $^1J_{CC}$ = 31−34 Hz.

**Kinetics of the Conversion of 5 to 6.** An NMR tube containing an equimolar solution of **5** and NCAr (42 mM) in $CD_2Cl_2$ was warmed at −41 °C and monitored periodically by $^1$H NMR spectroscopy. The

concentration of **5** was determined by integrating the carbomethoxy resonances of **5** ($\delta$ 3.69 and 3.43) versus the para phenyl proton of the $BAr_4^-$ counterion ($\delta$ 7.49). A plot of ln[**5**] vs time was linear to >3 half-lives with a first-order rate constant of $k = 5.04 \pm 0.05 \times 10^{-4}$ $s^{-1}$; two identical experiments gave an average value of $k = 5.2 \pm 0.8 \times 10^{-4}$ $s^{-1}$. The first-order rate constant for the conversion of **5** to **6** was determined at −62, −55, −51, and −30 °C (Table 1). A plot of ln *k*/T versus 1/*T* provided the activation parameters for the conversion of **5** to **6**; $\Delta H^{\ddagger} = 13.5 \pm 0.6$ kcal $mol^{-1}$, and $\Delta S^{\ddagger} = -15 \pm 2$ eu (Figure 3).

***trans,trans*-{(phen)Pd[CHCH(Me)CH($CH_2SiEt_3$)$CH_2$C(COOMe)-(COOMe)]}$^+$ $(BAr_4)^-$ (7).** Triethylsilane (12.3 $\mu$L, 0.077 mmol) was added via syringe to a solution of [(phen)Pd(Me)($NCCH_3$)]$^+$ $[BAr_4]^-$ (**2c**) (93 mg, 0.077 mmol) in $CH_2Cl_2$ (25 mL) at −78 °C, stirred for 30 min, and treated with **1** (16 $\mu$L, 0.077 mmol). The resulting solution was warmed to room temperature, stirred for 2 h, and concentrated under vacuum to form a yellow glass that was triturated with hexanes (3 × 5 mL) and dried under vacuum to give **7** (52 mg, 49%) as a yellow powder. $^1$H NMR resonances were assigned on the basis of $^1$H−$^1$H COSY analysis; the relative stereochemistry of **7** was assigned via degradation with $DSiEt_3$.

**For 7:** $^1$H NMR ($CDCl_3$, 23 °C): $\delta$ 8.92 (dd, $J = 1.4$, 4.9 Hz, 1 H, $H_c$), 8.85 (dd, $J = 1.4$, 5.4 Hz, 1 H, $H_c$), 8.64 (dd, $J = 1.2$, 8.2 Hz, 1 H, $H_a$), 8.62 (dd, $J = 1.6$, 8.4 Hz, 1 H, $H_a$), 8.07, 8.03 (ABq, $J = 8.9$ Hz, 2 H, $H_d$), 7.95 (dd, $J = 4.8$, 8.3 Hz, 1 H, $H_b$), 7.89 (dd, $J = 5.3$, 8.2 Hz, 1 H, $H_b$), 7.72 (t, $J = 2.4$ Hz, 8 H, $H_{o'}$), 7.55 (s, 4 H, $H_{p'}$), 4.16 (s, 3 H, $H_{13}$), 3.78 (s, 3 H, $H_{11}$), 2.85 (dd, $J = 7.1$, 13.0 Hz, 1 H, $H_4$), 2.47 (d, $J = 10.5$ Hz, 1 H, $H_1$), 1.70 (m, 1 H, $H_3$), 1.67 (d, $J = 12.8$ Hz, 1 H, $H_4$), 1.47 (m, 1 H, $H_2$), 1.20 (d, $J = 6.5$ Hz, 3 H, $H_6$), 1.06 (dd, $J = 2.4$, 14.4 Hz, 1 H, $H_7$), 0.97 (t, $J = 7.9$ Hz, 9 H, $H_9$), 0.58 (q, $J = 7.8$ Hz, 6 H, $H_8$), 0.37 (dd, $J = 11.2$, 14.4 Hz, 1 H, $H_7$). $^{13}$C{$^1$H} NMR ($CDCl_3$, 23 °C): $\delta$ 191.5 ($C_{12}$), 171.7 ($C_{10}$), 161.9 (q, $J_{CB} = 50.0$ Hz, $C_{i'}$), 151.7, 149.1 ($C_a$), 147.8, 143.8 ($C_e$), 139.7, 139.1 ($C_b$), 134.9 ($C_{o'}$), 130.9, 130.2 ($C_f$), 129.2 (q, $^2J_{CF} = 31.7$ Hz, $C_{m'}$), 128.0, 127.5, 126.0, 125.4 ($C_b$ and $C_c$), 124.6 (q, $^1J_{CF} = 272.8$ Hz, $C_{r'}$), 117.6 ($C_{p'}$), 68.5, 56.5, 53.8, 53.2, 42.1, ($C_1$, $C_2$, $C_5$, $C_{11}$, and $C_{13}$), 42.9, 40.9 ($C_3$ and $C_4$), 17.3 ($C_6$), 15.8 ($C_7$), 7.5 ($C_9$), 4.0 ($C_8$). IR (KBr, $cm^{-1}$): 1746, 1612 ($\nu_{C=O}$). Anal. Calcd (found) for $C_{61}H_{51}N_2O_4F_{24}PdSiB$: H, 3.48 (3.14); C, 49.59 (49.47); N, 1.90 (2.02).

**Reaction of 5 with $HSiEt_3$.** A solution of **5** (23 $\mu$mol, 43 mM) in $CD_2Cl_2$ (0.53 mL) was treated with $HSiEt_3$ (10.8 $\mu$L, 67.7 $\mu$mol) at −80 °C, shaken briefly, and placed in the probe of an NMR spectrometer pre-cooled at −81 °C. The NMR probe was warmed at −51 °C, and the solution was monitored periodically by $^1$H NMR spectroscopy. The concentration of **5** was determined by integrating the carbomethoxy resonances of **5** ($\delta$ 3.69 and 3.43) versus that of the para phenyl proton of the $BAr_4^-$ counterion ($\delta$ 7.49). A plot of ln[**5**] versus time was linear to 3 half-lives with a first-order rate constant of $k = 1.59 \pm 0.01 \times 10^{-4}$ $s^{-1}$ (Figure S2).

**Reaction of 6 with $HSiEt_3$.** A solution of **6** (~19 mmol, ~30 mM) in $CD_2Cl_2$ (0.60 mL) was treated with $HSiEt_3$ (30 $\mu$mol, 50 mM) at −78 °C, shaken briefly, and placed in the probe of an NMR spectrometer cooled at −80 °C. The NMR probe was warmed at −41 °C, and the solution was monitored periodically by $^1$H NMR. After 10 min, resonances corresponding to **6** could no longer be detected (≥95% conversion), and resonances corresponding to a 1:1 mixture of **4b** and **3** were observed.

**Reaction of 6 with $DSiEt_3$.** $DSiEt_3$ (5 $\mu$L, 31 $\mu$mol) was added via syringe to an NMR tube containing a solution of **6** (19 $\mu$mol) in $CD_2Cl_2$ (0.60 mL) at −80 °C. The tube was shaken briefly and placed in the probe of an NMR spectrometer pre-cooled at −41 °C. Upon complete consumption of **6** (~10 min), the sample was removed from the probe, and the solution was filtered through a plug of Celite and concentrated under vacuum to give **3**-$d_1$. Mass spectral analysis of **3**-$d_1$ indicated an isotopic purity of 98%, and $^1$H- and $^{13}$C NMR analysis revealed complete (≥95%) deuteration of the exocyclic methyl group. $^{13}$C{$^1$H} NMR ($CDCl_3$, 23 °C): $\delta$ 17.1 (t, $J = 19.1$ Hz, isotopic shift 300 ppb).

**Kinetics of the Silylation of 7.** A solution of **7** (22 $\mu$mol, 36 mM) and $HSiEt_3$ (0.21 mmol, 0.36 M) in $CD_2Cl_2$ (0.60 mL) was monitored periodically by $^1$H NMR spectroscopy at −14 °C. The concentration of **7** was determined by integrating the resonance corresponding to one of the carbomethoxy peaks of **7** ($\delta$ 4.24) relative to that of the para phenyl resonances of the $BAr_4^-$ counterion ($\delta$ 7.51). A plot of ln[**7**] versus time was linear to >4 half-lives (Figure S3), with a pseudo-first-order rate constant of $k_{obs} = 1.33 \pm 0.01 \times 10^{-4}$ $s^{-1}$. Employing a similar procedure, pseudo-first-order rate constants for the reaction of $HSiEt_3$ with **7** at −14 °C in $CD_2Cl_2$ were obtained at silane concentrations of 0.18, 0.20, 0.38, and 0.93 M (Table 2). For reactions employing initial silane concentrations of 0.18 and 0.20 M, the initial concentration of **7** was lowered to 20 mM. The resulting plot of $k_{obs}$ versus [$HSiEt_3$] was linear, which provided the second-order rate constant for silylation of **7** of $k = 3.3 \pm 0.3 \times 10^{-4}$ $M^{-1}$ $s^{-1}$ (Figure 4).

**Reaction of 7 with $DSiEt_3$.** $DSiEt_3$ (107 $\mu$L, 0.67 mmol) was added via syringe to a solution of **7** (160 mg, 0.13 mmol) in $CH_2Cl_2$ (1.6 mL) at room temperature, and the resulting solution was stirred for 2 h. The resulting black solution was concentrated under vacuum and chromatographed ($SiO_2$, hexanes−EtOAc = 24:1) to give *trans,trans*-1,1-dicarbomethoxy-2-deuterio-4-(triethylsilylmethyl)-3-methylcyclopentane (**3**-$d_1'$) as a colorless oil in 46% yield with 83% isotopic purity as determined by MS analysis. The regio- and stereochemistry of **3**-$d_1'$ was determined via $^1$H- and $^{13}$C NMR analysis and by comparison to the spectroscopy of unlabeled **3**; complete assignment of the $^1$H NMR resonances of **3** was achieved via combined $^1$H−$^1$H COSY and NOESY analysis. $^{13}$C{$^1$H} NMR ($CD_2Cl_2$, 23 °C): $\delta$ 42.0 [t, $J_{CD} = 20.6$ Hz, isotopic shift = 320 ppb, C(1)], 58.3 [s, isotopic shift = 60 ppb, C(5)], 43.8 [s, isotopic shift = 100 ppb, C(2)].

**Silane Competition Experiments.** A mixture of $HSiEt_3$ (4.95 mmol) and $HSiMe_2R$ (R = Et, *n*-octyl, $OSiMe_3$, or Ph) (4.95 mmol) was added via syringe to a solution of **1** (100 $\mu$L, 0.50 mmol) and a catalytic amount of **2b** (12 $\mu$mol) in DCE (10 mL) at 0 °C. The resulting solution was stirred at room temperature until **1** was completely consumed (as determined by GC analysis) to form a mixture of silylated carbocycles **3** and **3a**−**3d**, respectively. The ratio of carbocycles was determined by gas chromatography, correcting for the GC response factors of the carbocycles (Table 3). A second set of experiments employing a 1:1 mixture of $HSiMe_2Ph$ and $HSiMe_2(4\text{-}C_6H_4R)$ (R = $NMe_2$, OMe, $CF_3$, F) to form a mixture of silylated carbocycles **3d** and **3e**−**3h** was performed in an analogous manner (Table 3).

**Catalytic Cyclization/Deuteriosilylation.** A solution of **1** (100 $\mu$L, 0.50 mmol), (phen)PdMeCl (8 mg, 24 $\mu$mol), $NaBAr_4$ (23 mg, 26 $\mu$mol), and $DSiEt_3$ (300 $\mu$L, 1.9 mmol) in DCE (10 mL) was stirred at room temperature for 30 min. The resulting dark solution was concentrated and chromatographed ($SiO_2$, hexanes−EtOAc = 24:1) to give **3**-$d_1$ (167 mg, 102%) as a colorless oil. Mass spectral analysis indicated an isotopic purity of 98%, and $^1$H- and $^{13}$C NMR analysis revealed complete (≥95%) deuteration of the exocyclic methyl group.

**Kinetics of Catalytic Cyclization/Hydrosilylation.** $CD_2Cl_2$ (0.58 mL), NCAr (2.98 $\mu$L, 17.7 $\mu$mol), and **1** (10.0 $\mu$L, 49.5 $\mu$mol) were added sequentially via syringe to a 5-mm NMR tube containing **2b** (9.9 mg, 7.0 $\mu$mol) that was sealed with a septum. After the tube was shaken thoroughly and cooled at −81 °C, $HSiEt_3$ (16 $\mu$L, 100 $\mu$mol) was added via syringe and the tube was placed in the probe of an NMR spectrometer pre-cooled at −80 °C. The sample was then warmed at −41 °C and monitored periodically by $^1$H NMR spectroscopy. The concentration of **1** was determined by integrating the olefinic resonances of **1** at $\delta$ 5.08 and 5.11 relative to the aryl para hydrogen resonance of $BAr_4^-$ at $\delta$ 7.52. A plot of [**1**] versus time was linear to 3 half-lives (Figure 6), with an observed rate constant of $k_{obs} = 8.20 \pm 0.04 \times 10^{-6}$ M $s^{-1}$; two identical experiments gave an average value of $k_{obs} =$

$8.3 \pm 0.6 \times 10^{-6}$ M $s^{-1}$ (Table 4, entries 1−3). Resonances attributed to the olefinic protons [$\delta$ 6.41 (dtd, $J$ = 4.3, 8.4, 16.1 Hz, 1 H, −C*H*═$CH_2$), 5.44 (d, $J$ = 9.0 Hz, 1 H, −CH═C$H_2$), 4.22 (d, $J$ = 16.1 Hz, 1 H, −CH═C$H_2$)] and carbomethoxy protons [3.68 (s, 3 H), and 3.43 (s, 3 H)] of **5** were observed throughout complete conversion of **1** to **3**. Pseudo-zero-order rate constants for the reaction of **1** ($[\mathbf{1}]_0$ = 85 mM) and $HSiEt_3$ ($[HSiEt_3]_0$ = 0.16 M) catalyzed by **2b** were determined as a function of [NCAr], [**2b**], and temperature, employing a similar procedure (Table 4). The first-order rate constant for the catalytic cyclization/hydrosilylation of **1** ($[\mathbf{1}]_0$ = 85 mM) and $HSiEt_3$ ($[HSiEt_3]_0$ = 0.16 M) at −41 °C was determined from the linear plot of pseudo-zero-order rate constants versus $[\mathbf{2b}]_0$ over the range 0−25 mM (Figure 7). The activation parameters for the reaction of **1** ($[\mathbf{1}]_0$ = 85 mM) and $HSiEt_3$ ($[HSiEt_3]_0$ = 0.16 M) catalyzed by **2b** ($[\mathbf{2b}]_0$ = 12 mM) were obtained from a plot of ln $k/T$ versus $1/T$ over the range −57 to −25 °C (Figure 8). The dependence of the rate of catalytic cyclization/hydrosilylation on silane concentration was determined via iterative fitting of two sets of concentration versus time data for reaction of **1** ($[\mathbf{1}]_0$ = 85 mM), **2b** ($[\mathbf{2b}]_0$ = 12 mM), and $HSiEt_3$ ($[HSiEt_3]_0$ = 90 mM) in $CD_2Cl_2$ that contained NCAr (42 mM) at −41 °C to the rate equation depicted in eq 2 employing MacKinetics (version 0.9.1b). This analysis provided a best fit with $k_2 = 7.6 \pm 0.2 \times 10^{-4}$ $s^{-1}$ and $k_3 = 0.12 \pm 0.03$ $M^{-1}$ $s^{-1}$. To estimate the error limit for $k_3$, $k_2$ was held constant ($k_2 = 7.6 \times 10^{-4}$ $s^{-1}$), $k_3$ was incrementally varied by ±0.01 $M^{-1}$ $s^{-1}$, and the resulting concentration versus time plots were compared visually to the experimental data. The error limit for $k_2$ determined via iterative fitting was estimated by employing an analogous procedure.

**Acknowledgment** is made to the NIH (GM59830-01) and PRF (36399-AC4), administered by the American Chemical Society, for support of this research. We thank Mr. Jeff Cross (UNC-Chapel Hill) for obtaining the $^{13}C$ NMR spectra of **5**-$^{13}C_6$ and **6**-$^{13}C_6$, and Dr. Tao Pei for synthesizing **1**-1,2,3,5,6,7-$^{13}C_6$ and **1**-3,3,5,5-$d_4$.

**Supporting Information Available:** Syntheses and spectral data for **1a**-$^{13}C_3$, **1**-1,2,3,5,6,7-$^{13}C_6$, **5**-$d_2$, **5**-$d_4$, **6**-$d_2$, and **6**-$d_4$, spectral and analytical data for **3b**, **3e**, **3f**, **3g**, and **3h**, and representative kinetic plots for reaction of **5** and **7** with $HSiEt_3$ and for the conversion of **6** to **7**. This material is available free of charge via the Internet at http://pubs.acs.org.

JA049806F